

1 **Cold-induced  $[Ca^{2+}]_{cyt}$  elevations function to support osmoregulation in marine diatoms**

2

3 Friedrich H. Kleiner<sup>1,2</sup>, Katherine E. Helliwell<sup>1,3</sup>, Abdul Chrachri<sup>1</sup>, Amanda Hopes<sup>4</sup>, Hannah  
4 Parry-Wilson<sup>1,2</sup>, Trupti Gaikwad<sup>1</sup>, Nova Mieszkowska<sup>1,5</sup>, Abdul Chrachri<sup>1</sup>, Thomas Mock<sup>4</sup>,  
5 Glen L. Wheeler<sup>1\*</sup>, Colin Brownlee<sup>1\*</sup>

6

7

8 1 The Marine Biological Association of the United Kingdom, The Laboratory, Citadel Hill,  
9 Plymouth, Devon, PL1 2PB, UK

10 2 School of Ocean and Earth Science, University of Southampton, Southampton, SO14 3ZH,  
11 UK

12 3 Biosciences, College of Life and Environmental Sciences, University of Exeter, Exeter EX4  
13 4QD, UK

14 4 School of Environmental Sciences, University of East Anglia, Norwich Research Park,  
15 Norwich, UK

16 5 School of Environmental Sciences, University of Liverpool, Jane Herdman Building,  
17 Liverpool, L69 3GP, UK

18

19

20

21 \*Corresponding authors: [glw@mba.ac.uk](mailto:glw@mba.ac.uk), [cbr@mba.ac.uk](mailto:cbr@mba.ac.uk)

22

23 **Abstract**

24

25 Diatoms are a group of microalgae that are important primary producers in a range of open  
26 ocean, freshwater and intertidal environments. The latter can experience significant long- and  
27 short-term variability in temperature, from seasonal variations to rapid temperature shifts  
28 caused by tidal immersion and emersion. As temperature is a major determinant in the  
29 distribution of diatom species, their temperature sensory and response mechanisms likely  
30 have important roles in their ecological success. We have examined the mechanisms diatoms  
31 use to sense rapid changes in temperature, such as those experienced in the intertidal zone.  
32 We find that the diatoms *Phaeodactylum tricornutum* and *Thalassiosira pseudonana* exhibit a  
33 transient cytosolic  $\text{Ca}^{2+}$  ( $[\text{Ca}^{2+}]_{\text{cyt}}$ ) elevation in response to rapid cooling, similar to those  
34 observed in plant and animal cells. However,  $[\text{Ca}^{2+}]_{\text{cyt}}$  elevations were not observed in  
35 response to rapid warming. The kinetics and magnitude of cold-induced  $[\text{Ca}^{2+}]_{\text{cyt}}$  elevations  
36 correlate with the rate of temperature decrease. We do not find a role for the  $[\text{Ca}^{2+}]_{\text{cyt}}$   
37 elevations in enhancing cold tolerance, but show that cold shock induces a  $\text{Ca}^{2+}$ -dependent  $\text{K}^+$   
38 efflux and reduces mortality of *P. tricornutum* during a simultaneous hypo-osmotic shock. As  
39 inter-tidal diatom species may routinely encounter simultaneous cold and hypo-osmotic  
40 shocks during tidal cycles, we propose that cold-induced  $\text{Ca}^{2+}$  signalling interacts with  
41 osmotic signalling pathways to aid in the regulation of cell volume. Our findings provide  
42 insight into the nature of temperature perception in diatoms and highlight that cross-talk  
43 between signalling pathways may play an important role in their cellular responses to multiple  
44 simultaneous stressors.

45

## 46 **Introduction**

47 Diatoms are a group of silicified unicellular algae that represent one of the most important  
48 primary producers in modern oceans. They are abundant in diverse marine environments,  
49 most notably in polar and temperate upwelling regions, where they play a critical role at the  
50 base of the marine food web (Malviya et al., 2016). Diatom communities are abundant across  
51 a broad temperature range in the surface ocean from sea ice to tropical oceans. Diatoms are  
52 also important primary producers in freshwater and brackish ecosystems, where they likely  
53 encounter an even greater range of temperatures (Souffreau et al., 2010).

54 Global rises in surface temperature due to anthropogenic CO<sub>2</sub> emissions are set to have  
55 profound influence on marine ecosystems (Gattuso et al., 2015). These future changes in our  
56 climate will also increase the variability of temperature regimes and the prevalence of extreme  
57 events, such as marine heatwaves, that may co-occur with other stressors such as low pH or  
58 deoxygenation (Harley et al., 2006; Smale et al., 2019; Gruber et al., 2021). Understanding  
59 the physiological response of diatoms and other marine phytoplankton to changes in global  
60 temperature regimes is therefore of the utmost importance. Temperature has an important  
61 impact on diatom cell physiology, influencing cell size and formation of the silica frustule  
62 (Montagnes and Franklin, 2001; Svensson et al., 2014; Javaheri et al., 2015). Individual  
63 species display a thermal niche with distinct temperature growth optima that reflect their  
64 natural environment (Liang et al., 2019). The upper and lower thermal tolerance limits, rather  
65 than the optima themselves, appear to have the greatest influence on the distribution of  
66 individual diatom species (Anderson and Rynearson, 2020), with temperatures in excess of  
67 the upper thermal tolerance limits leading to a rapid increase in the rates of cell death (Baker  
68 and Geider, 2021).

69 Many of these studies have focussed on the physiological responses of diatoms to longer term  
70 changes in temperature. However, diatoms will also experience short term temperature  
71 variations within their natural habitat. This is particularly so for those species that inhabit  
72 intertidal rocky shores or estuarine habitats where immersion and emersion is associated with  
73 rapid and regular temperature fluctuations. Rapid temperature changes are potentially highly  
74 damaging to diatom cells, demonstrated by their much greater vulnerability to abrupt rather  
75 than gradual temperature increases (Souffreau et al., 2010). Temperature variability may also  
76 have an important influence on the ability of diatoms to adapt to their thermal niche, as  
77 *Thalassiosira pseudonana* exhibited accelerated adaptation to higher temperatures under a  
78 fluctuating temperature regime (Schaum et al., 2018). Despite the importance of thermal

79 tolerance in diatom physiology and ecology, relatively little is known about the physiological  
80 mechanisms that allow diatoms to perceive and respond to changes in temperature,  
81 particularly during short-term fluctuations.

82 Many of the cellular mechanisms involved in temperature sensing in eukaryotes involve  
83 temperature-induced changes in the structure of nucleic acids, proteins or biological  
84 membranes that lead to a range of downstream physiological responses (Sengupta and  
85 Garrity, 2013).  $\text{Ca}^{2+}$ -dependent signalling mechanisms play an important role in these  
86 temperature sensing pathways. In animal cells, heat stress is associated with  $\text{Ca}^{2+}$  influx into  
87 the cytosol via the TRPV family of temperature-sensitive ion channels (Xu et al., 2002;  
88 Clapham and Miller, 2011).  $\text{Ca}^{2+}$  signalling also plays a role in sensing low temperature in  
89 animals, for example underpinning the rapid cold hardening response of insects (Teets et al.,  
90 2013). Land plants also employ  $\text{Ca}^{2+}$  signalling mechanisms in their response to both low and  
91 high temperatures. Rapid cooling of plants induces a transient cytosolic  $\text{Ca}^{2+}$  ( $[\text{Ca}^{2+}]_{\text{cyt}}$ )  
92 elevation, which leads to changes in gene expression and the establishment of cold tolerance  
93 (Knight et al., 1996; Tahtiharju et al., 1997; Knight and Knight, 2012). Some plants, such as  
94 the moss *Physcomitrium*, also display  $[\text{Ca}^{2+}]_{\text{cyt}}$  elevations in response to heat shock (Saidi et  
95 al., 2009). In other plants, such as *Arabidopsis*, high temperatures do not induce  $[\text{Ca}^{2+}]_{\text{cyt}}$   
96 elevations, although  $\text{Ca}^{2+}$  elevations are observed within the chloroplast (Lenzoni and Knight,  
97 2019). Potential temperature sensors in plants include the cold sensitive COLD1/RGA1  
98 complex in *Oryza sativa*, which is proposed to either function as a  $\text{Ca}^{2+}$  channel or to activate  
99 other  $\text{Ca}^{2+}$  channels (Ma et al., 2015). Specific cyclic nucleotide-gated ion channels and  
100 annexins may also play a role in temperature sensing pathways, with mutant strains in  
101 *Physcomitrium*, *O. sativa* and *Arabidopsis* exhibiting diminished  $[\text{Ca}^{2+}]_{\text{cyt}}$  elevations in  
102 response to cold- and heat shock (Cui et al., 2020; Liu et al., 2021). However, it is currently  
103 unclear whether these ion channels sense temperature directly or are activated indirectly, e.g.  
104 through changes in membrane rigidity (Plieth et al., 1999) or the cytoskeleton (Pokorna et al.,  
105 2004).

106 Our understanding of  $\text{Ca}^{2+}$  signalling in diatoms remains in its infancy, although  $\text{Ca}^{2+}$ -  
107 dependent signalling mechanisms have been identified in response to a range of  
108 environmental stimuli, such as the supply of nutrients (phosphate and iron), hypo-osmotic  
109 shock and the detection of toxic aldehydes (Falciatore et al., 2000; Vardi et al., 2006;  
110 Helliwell et al., 2021; Helliwell et al., 2021). Initial experiments using *Phaeodactylum*  
111 *tricornutum* cells expressing the bioluminescent  $\text{Ca}^{2+}$  reporter aequorin did not detect  $[\text{Ca}^{2+}]_{\text{cyt}}$

112 elevations in response to low (4 °C) or high (37 °C) temperature (Falciatore et al., 2000).  
113 More recently, genetically-encoded fluorescent Ca<sup>2+</sup> reporters have been successfully  
114 expressed in *P. tricornutum* and *T. pseudonana*, enabling high resolution imaging of [Ca<sup>2+</sup>]<sub>cyt</sub>  
115 elevations in single diatom cells (Helliwell et al., 2021; Helliwell et al., 2021). These  
116 advances will now allow detailed examination of diatom signalling in response to range of  
117 stimuli, including temperature.

118 In this study we set out to examine the ability of diatoms to sense short-term changes in  
119 temperature. In particular, we examined whether the well-characterised [Ca<sup>2+</sup>]<sub>cyt</sub> elevations  
120 observed in animal and plant cells in response to rapid changes in temperature were conserved  
121 in diatoms. Using the model species *P. tricornutum* and *T. pseudonana*, which can both  
122 inhabit coastal environments that experience variable temperature regimes (De Martino et al.,  
123 2007; Alverson et al., 2011), we found that diatoms consistently exhibit a [Ca<sup>2+</sup>]<sub>cyt</sub> elevation  
124 in response to cold shock, but do not exhibit [Ca<sup>2+</sup>]<sub>cyt</sub> elevations in response to elevated  
125 temperature. We did not find a requirement for cold shock-induced Ca<sup>2+</sup> signalling in  
126 increasing tolerance to low temperatures, but found that cold shock increases resistance to  
127 simultaneous hypo-osmotic shocks, suggesting that integration of multiple signalling inputs  
128 may contribute to an enhanced ability to respond to these environmental stimuli.

129

## 130 **Methods**

### 131 Recording of rockpool temperature

132 Temperature data was recorded using a 27 mm Envlogger v2.4 (ElectricBlue, Porto, Portugal)  
133 encased in acrylic resin, recording in 30 minute intervals with a resolution of 0.1 °C. The  
134 Envlogger was secured to the substrate using Z-Spar A-788 epoxy resin roughly 3 cm below  
135 the surface waters of a shallow midshore rockpool measuring approximately 8 cm deep at  
136 Looe Hannfore, Cornwall, UK (50.3411, -4.4598) from 1/7/2019 to 7/7/2019.

### 137 Strains and culturing conditions

138 The wild type *P. tricornutum* strain used in this study was CCAP 1055/1 (Culture Collection  
139 of Algae and Protozoa, SAMS, Scottish Marine Institute, Oban, UK). A *P. tricornutum* strain  
140 transformed with the R-GECO1 Ca<sup>2+</sup> biosensor (PtR1) and the three *eukcatal* knock-out  
141 strains in this line (labelled A3, B3 and B6) were generated as described previously (Helliwell  
142 et al., 2019). The *T. pseudonana* strain expressing the R-GECO1 biosensor (TpR1) was  
143 generated as described in Helliwell et al (2021). Cultures were maintained in natural seawater  
144 with f/2 nutrients (J C Lewin and Guillard, 1963; Guillard, 1975); modified by the addition of  
145 106 µM Na<sub>2</sub>SiO<sub>3</sub>·5H<sub>2</sub>O and the exclusion of vitamins (*P. tricornutum* only). For imaging  
146 experiments, cells were acclimated to an artificial seawater (ASW) medium for minimum 10  
147 days prior to analysis. ASW contained 450 mM NaCl, 30 mM MgCl<sub>2</sub>, 16 mM MgSO<sub>4</sub>, 8 mM  
148 KCl, 10 mM CaCl<sub>2</sub>, 2 mM NaHCO<sub>3</sub>, 97 µM H<sub>3</sub>BO<sub>3</sub>, f/2 supplements and 20 mM HEPES (pH  
149 8.0). Cultures were grown at 18 °C with a 16:8 light/dark cycle under illumination of 50 µmol  
150 m<sup>-2</sup> s<sup>-1</sup>.

### 151 Epifluorescence imaging of R-GECO1 fluorescence

152 500 µL of cell culture was added to a 35 mm microscope dish with glass coverslip base (In  
153 Vitro Scientific, Sunnyvale, CA, USA) coated with 0.01% poly-L-lysine (Merck Life Science  
154 UK, Gillingham, Dorset) to promote cell adhesion to the glass surface. Cells were allowed to  
155 settle for 5-20 minutes at room temperature (RT) under light. R-GECO1 was imaged using a  
156 Leica DMI8 inverted microscope (Leica Microsystems, Milton Keynes, UK) with a 63x  
157 1.4NA oil immersion objective, using a Lumencor SpectraX light source with a 541-551 nm  
158 excitation filter and 565-605 nm emission filter. Images were captured with a Photometrics  
159 Prime 95B sCMOS camera (Teledyne Photometrics, Birmingham, UK). Images were  
160 captured at 3.33 frames per second using Leica application suite X-software v.3.3.0.

161 Administration of temperature shocks to cells in the imaging setup

162 The dish was perfused with ASW without f/2 nutrients at a standard flow rate of 16 mL min<sup>-1</sup>.  
163 To achieve rapid changes in temperature in the dish, the perfusion was switched between  
164 solutions of different temperature to achieve target temperatures of approximately 10, 22 or  
165 30 °C respectively. Actual dish temperature was recorded using a Firesting micro optical  
166 temperature sensor (Pyroscience GmbH, Aachen, Germany). For the majority of experiments,  
167 cells were perfused with warmer media (dish temperature 30 °C) for 1 minute prior to  
168 application of the cooling shock (these conditions reflect those observed in the rockpool  
169 observations). The perfusion flow rate was altered to achieve different temperature change  
170 rates. As cooling rate was not linear, the maximum cooling rate was defined as the largest  
171 decrease temperature within a one second period.

172 Application of inhibitors and elicitors

173 External Ca<sup>2+</sup> was removed by perfusion with ASW without CaCl<sub>2</sub> containing 200 μM EGTA.  
174 Ruthenium red (RR) was added to cells at a final concentration of 10 μM 5 minutes prior to  
175 cold shock treatment. Menthol was prepared as a 1 M stock solution in DMSO and used at  
176 concentration of 1 mM, resulting in a final DMSO concentration of 0.1%.

177 Processing of imaging data

178 Images were processed using LasX software (Leica). The mean fluorescence intensity within  
179 a region of interest (ROI) over time was measured for each cell by drawing an ROI  
180 encompassing the whole cell. Background fluorescence was subtracted from all cellular F  
181 values. The change in the fluorescence intensity of R-GECO1 was then calculated by  
182 normalizing each frame by the initial value (F/F<sub>0</sub>). [Ca<sup>2+</sup>]<sub>cyt</sub> elevations were defined as any  
183 increase in F/F<sub>0</sub> above a threshold value (1.5). The duration of a [Ca<sup>2+</sup>]<sub>cyt</sub> elevation was defined  
184 as the peak width at half maximal amplitude. To visualise the spatial distribution of a [Ca<sup>2+</sup>]<sub>cyt</sub>  
185 elevation, each frame was divided by a corresponding background image generated by  
186 applying a rolling median (30 frames) to the image-series (Image J). The resultant time series  
187 images were pseudo-coloured to indicate changes in fluorescence.

188 Statistical analysis

189 Graphs and statistical analyses were performed using Sigmaplot v14.0 (Systat Software,  
190 Slough, UK). Error bars represent standard error of the mean. Unless indicated otherwise,

191 imaging experiments were repeated three times with independent cultures on different days to  
192 ensure reproducibility of the response.

193 Normal distribution of respective datasets was tested using Shapiro-Wilk's normality test.  
194 When passed, statistical analysis of datasets with two groups were done with Student's t-test,  
195 and when not passed with Mann-Whitney's rank sum test. Statistical analysis of datasets with  
196 more than two groups were performed using an ANOVA followed by a Holm-Sidak post-hoc  
197 test when the normality test was positive. When the normality test was negative, Kruskal-  
198 Wallis' 1-way Analysis of Variance on Ranks was used instead. All statistical tests were  
199 performed with Sigmaplot v14.0.3.192 (Systat software Inc).

#### 200 Growth at different temperatures after a cold shock.

201 For the growth curves, cells were grown to mid exponential phase ( $2.73 \times 10^6$  cells mL<sup>-1</sup>). The  
202 culture was divided into 10 mL aliquots and cells were pelleted by centrifugation (4000 x g at  
203 18 °C). Cells were washed in 40 mL ASW +/- Ca<sup>2+</sup> and pelleted again by centrifugation. Cells  
204 were then resuspended in their respective treatments (20 mL of ASW +/- Ca<sup>2+</sup> at 18 °C or 4  
205 °C to administer a rapid cold shock). After 10 minutes, 2 mL of each culture was used to  
206 inoculate culture vessels containing 18 mL of standard F/2 media (approx. starting density of  
207  $6.8 \times 10^4$  cells mL<sup>-1</sup>) and cultures were grown at 18 °C or 4 °C.

#### 208 Cell survival during hypo-osmotic shock

209 To examine the effect of temperature on cell viability during hypo-osmotic shock, 10 mL of a  
210 late log phase culture ( $6 \times 10^6$  cells mL<sup>-1</sup>) were pelleted by centrifugation (4000 x g at 18 °C).  
211 Cells were washed twice with 10 mL ASW +/-Ca<sup>2+</sup> and 250 µL aliquots were taken. To apply  
212 the hypo-osmotic and cold shock treatments, 750 µL of ASW (+/- Ca<sup>2+</sup>) or deionised water at  
213 two different temperatures (20 °C or 4 °C) were added to each tube. Addition of water results  
214 in a severe hypo-osmotic osmotic shock (final concentration 25% ASW) simultaneously with  
215 the temperature shock. The cells were then incubated at their respective temperatures for 3  
216 minutes prior to addition of 5 µM Sytox Green (Thermo Fisher Scientific, Loughborough,  
217 UK). All treatments were then incubated at 20 °C 15 min in darkness. Cell viability was  
218 measured with a LUNA-FL™ Dual Fluorescence Cell Counter (Logos Biosystems, Villeneuve  
219 d'Ascq, France) to count live (displaying red chlorophyll fluorescence) versus dead cells  
220 (Sytox Green stain) with following settings: Excitation intensity green = 11, red = 7, count  
221 threshold for both = 3.



222 Quantification of K<sup>+</sup> efflux in *P. tricornutum* populations using K<sup>+</sup> -selective microelectrodes

223 K<sup>+</sup> microelectrodes were fabricated as described previously (Helliwell et al., 2021). Clark  
224 GC-1.5 borosilicate glass capillaries (Harvard Apparatus, Cambridge, UK) were pulled to a  
225 fine point using a P-97 pipette puller (Sutter, Novato, CA). The pipette tips were then gently  
226 broken to produce a diameter of ca 10-20 μm. The capillaries were silanised by exposure to  
227 N,N-dimethyltrimethylsilylamine (TMSDMA) vapour at 200 °C for 20 minutes within a  
228 closed glass Petri dish. The K<sup>+</sup> microelectrodes were prepared by introducing K<sup>+</sup> ionophore I  
229 (Sigma Aldrich, Gillingham, Dorset, UK) into the pipette tip by suction. Pipettes were then  
230 back-filled with the filling solution (100 mM NaCl, 20 mM HEPES pH 7.2 and 10 mM  
231 NaOH). The reference electrode was filled with 3 M KCl and data were recorded using an  
232 AxoClamp 2B amplifier, with pClamp v10.6 software (Molecular Devices, CA, USA). Each  
233 K<sup>+</sup> microelectrode was calibrated using a two-point calibration with standard KCl solutions.  
234 The mean slope of the calibrated electrodes was 53.0 ± 1.3 mV per decade (±SE).

235 For the measurements, 10 mL of *P. tricornutum* cells from exponential culture containing 10<sup>6</sup>-  
236 10<sup>7</sup> cells mL<sup>-1</sup> were centrifuged at 4000 rpm for 10 min and re-suspended in 1 mL of ASW.  
237 The cells were then allowed to settle on a poly-L-lysine coated microscope dish. Cells were  
238 perfused with ASW or ASW -Ca<sup>2+</sup> (0 μM Ca<sup>2+</sup> + 100 μM EGTA) and cold shocks were  
239 applied as described for the microscopy observations. Control experiments were performed in  
240 the absence of *P. tricornutum* cells to ensure that the change in temperature did not alter the  
241 performance of the K<sup>+</sup> microelectrodes.

242

## 243 **Results**

### 244 **Rapid changes in temperature in inter-tidal environments**

245 *P. tricornutum* was first isolated from a tidal pool in the UK and has since been identified in a  
246 range of coastal and brackish habitats (De Martino et al., 2007). To assess the dynamic  
247 temperature regimes potentially experienced by intertidal diatoms, we measured the  
248 temperature of a tidal pool located on the upper region of a rocky shore (South Cornwall, UK)  
249 over a 7 d period during July (UK summer). Temperatures within the pool were very stable  
250 around 15°C during immersion at high tide (Fig 1). However, at low tides temperatures in the  
251 exposed tidal pool rose significantly during the day (up to 30 °C) and decreased at night (to  
252 12 °C), before being rapidly restored to the bulk seawater temperature by the immersion of  
253 the pool at high tide. These data illustrate that diatoms inhabiting intertidal environments in  
254 temperate regions will regularly experience periods of significant warming followed by rapid  
255 cooling. The fluctuations in temperature are likely to be even greater in smaller volumes of  
256 water, such as the surface of estuarine mudflats or very shallow pools.

### 257 **Calcium signalling in response to changes in temperature**

258 *P. tricornutum* cells expressing the R-GECO1 Ca<sup>2+</sup> biosensor were perfused with seawater at  
259 high or low target temperatures (30 °C or 12 °C). Note that actual temperatures in the  
260 perfusion dish differed by ± 2 °C from these target temperatures due to equilibration of the  
261 small volume of warm or cold perfusate with room temperature. Actual dish temperatures  
262 were therefore recorded and are displayed for all experiments. We routinely observed a single  
263 transient [Ca<sup>2+</sup>]<sub>cyt</sub> elevation in cells exposed to a cold shock from 30 °C to 12 °C (97 % cells,  
264 n=63) (Fig 2A). In contrast, cells exposed to a rapid rise in temperature from 12 °C to 30 °C  
265 did not show [Ca<sup>2+</sup>]<sub>cyt</sub> elevations (Fig. 2A). No [Ca<sup>2+</sup>]<sub>cyt</sub> elevations were observed in cells  
266 perfused with these solutions after they had been equilibrated to room temperature, indicating  
267 that the act of switching between the perfusion solutions does not contribute to the signalling  
268 responses (Fig. 2A). Analysis of the spatial characteristics of cold-shock induced [Ca<sup>2+</sup>]<sub>cyt</sub>  
269 elevations indicated that many initiate at the apex of the cell and propagate towards the  
270 central region (Fig 2B), in a manner similar to those induced by mild hypo-osmotic shock  
271 (Helliwell et al., 2021). This suggests that the apices of the cell may play an important role in  
272 sensing the temperature changes. Cells exposed to a second cold shock two minutes after a  
273 previous cold shock demonstrated [Ca<sup>2+</sup>]<sub>cyt</sub> elevations with no significant attenuation in  
274 amplitude, although the percentage of cells responding was slightly lower (97% to 81 % of  
275 cells, n=63) (Supplementary Fig S1).

276 The  $[Ca^{2+}]_{cyt}$  elevations observed during cold shock were represented by a >10-fold increase  
277 in R-GECO1 fluorescence. Assuming a  $K_d$  of 480 nM for R-GECO1 and comparison with  
278 published maximum  $F/F_0$  values (Zhao et al., 2011), we estimate that  $[Ca^{2+}]_{cyt}$  elevations  
279 reach concentrations in the  $\mu M$  range, which are likely to be physiologically significant. In  
280 addition to these large increases in fluorescence that are attributed to  $[Ca^{2+}]_{cyt}$  elevations,  
281 much smaller changes in the baseline fluorescence of each cell could be observed following  
282 changes in temperature (increasing with low temperature and decreasing with high  
283 temperature, Supplemental Fig S1). These minor changes most likely represent temperature-  
284 dependent changes in R-GECO1 fluorescence emission (Ohkura et al., 2012) rather than  
285 actual changes in resting  $Ca^{2+}$  concentration. Therefore, only the substantial transient  
286 increases in fluorescence ( $F/F_0 > 1.5$ ) representing large  $[Ca^{2+}]_{cyt}$  elevations were analysed  
287 further.

288  $[Ca^{2+}]_{cyt}$  elevations were also observed when a cold shock (30°C to 12 °C) was applied to  
289 cells held at 22 °C, rather than 30 °C, indicating that the cold shock response was not a  
290 consequence of prior warming of the cells (Supplemental Fig S2). The percentage of cells  
291 responding to cold shock was lower in cells held at 22 °C compared to cells held at 30 °C,  
292 although this may also be influenced by the lower maximum rate of cooling at 22 °C.

293

#### 294 **Rapid cooling is required to elicit a $[Ca^{2+}]_{cyt}$ elevation**

295 We therefore examined the nature of the temperature change required to elicit  $[Ca^{2+}]_{cyt}$   
296 elevations, by manipulating the flow rate of the perfusion to vary the rate of cooling. Rapid  
297 cooling (2.5 °C s<sup>-1</sup>) resulted in  $[Ca^{2+}]_{cyt}$  elevations in 100% of cells examined (n=45), whereas  
298 only 7% of cells exhibited a  $[Ca^{2+}]_{cyt}$  elevation at a cooling rate of 0.4 °C s<sup>-1</sup> (n=45) (Fig. 3A-  
299 B). The amplitude of the  $[Ca^{2+}]_{cyt}$  elevations in responding cells closely correlated with the  
300 cooling rate, with much larger  $[Ca^{2+}]_{cyt}$  elevations observed at rapid cooling rates (Fig. 3C).  
301 Examination of a broader range of cooling rates indicated that a cooling rate greater than 1 °C  
302 s<sup>-1</sup> was required to elicit  $[Ca^{2+}]_{cyt}$  elevations in 50% of the population (Fig. 3D). These data  
303 suggest that the cold shock-induced  $[Ca^{2+}]_{cyt}$  elevations can therefore relay information  
304 relating to the nature of the stimulus both in terms of the number of cells responding and the  
305 nature of the  $[Ca^{2+}]_{cyt}$  elevation itself.

306 As very low perfusion rates also resulted in a lower overall decrease in temperature (due to  
307 equilibration of the perfusate with room temperature), we next examined the absolute

308 temperature decrease required to initiate signalling. Cells were perfused at 30 °C for 1 minute  
309 and then perfused at a constant flow rate with cold ASW (4 °C) for different durations to vary  
310 the decrease in temperature whilst maintaining similar rates of cooling. A very brief perfusion  
311 (4 s) lowered the temperature by  $2.4 \pm 0.6$  °C but did not induce  $[Ca^{2+}]_{cyt}$  elevations (Fig 3E-  
312 F). However, the rate of cooling in this treatment was considerably lower than the other  
313 treatments, due to buffering of the temperature by the residual volume within the perfusion  
314 dish (1 mL). Perfusions of a longer duration (7-26 s) resulted in a consistent cooling rate of  
315  $2.1-2.4$  °C  $s^{-1}$ . A temperature decrease of  $8.8 \pm 0.4$  °C induced a  $[Ca^{2+}]_{cyt}$  elevation in 38.4%  
316 of cells (n=126), whereas greater decreases in temperature resulted in  $[Ca^{2+}]_{cyt}$  elevations in  
317 nearly all cells (Fig. 3E-F). The amplitude and duration of  $[Ca^{2+}]_{cyt}$  elevations increased with  
318 the greater duration of the temperature decrease (Fig 3G-H). A cooling duration of 26 s did  
319 not increase the amplitude of the  $[Ca^{2+}]_{cyt}$  elevation beyond those observed at 9 s, but greatly  
320 increased the duration of the  $[Ca^{2+}]_{cyt}$  elevation (Fig 3G-H). Taken together, our results show  
321 that the cooling rate and the duration of the cold shock influence the amplitude and duration  
322 of the  $[Ca^{2+}]_{cyt}$  elevation and the percentage of cells responding.

323

### 324 **The cold shock response is conserved in the centric diatom *T. pseudonana* but displays** 325 **different characteristics**

326 *T. pseudonana* is a planktonic centric diatom found in marine, estuarine and freshwater  
327 environments (Alverson et al., 2011), where it is also likely to be exposed to significant  
328 changes in temperature. We found that *T. pseudonana* cells expressing the R-GECO1  
329 biosensor exhibited  $[Ca^{2+}]_{cyt}$  elevations in response to cold shock, with the amplitude of these  
330 elevations also dependent on the rate of temperature decrease (Fig. 4A-B). As in *P.*  
331 *tricornutum*, a control perfusion using ASW media equilibrated to room temperature did not  
332 induce  $[Ca^{2+}]_{cyt}$  elevations (Fig. 4C). The cold induced  $[Ca^{2+}]_{cyt}$  elevations in *T. pseudonana*  
333 were of a lower amplitude but longer duration than those observed in *P. tricornutum*. The  
334 percentage of *T. pseudonana* cells responding to cold shock was also considerably lower than  
335 *P. tricornutum* (19 % vs. 81 %, respectively), although variable levels of expression of R-  
336 GECO1 in *T. pseudonana* likely prevented detection of  $[Ca^{2+}]_{cyt}$  elevations in all cells within  
337 a field of view (Helliwell et al., 2021) (Fig. 4D-F). Taken together, these findings suggest that  
338 cold shock-induced  $[Ca^{2+}]_{cyt}$  elevations are exhibited by both pennate and centric diatom  
339 lineages and may therefore represent a conserved mechanism in many diatom species.

340

## 341 Cellular mechanisms underlying the cold shock response

342 We next examined the cellular mechanisms responsible for cold shock  $\text{Ca}^{2+}$  signalling in *P.*  
343 *tricornutum*. Removal of external  $\text{Ca}^{2+}$  by perfusion of PtR1 cells with cold  $\text{Ca}^{2+}$ -free ASW  
344 completely abolished the  $[\text{Ca}^{2+}]_{\text{cyt}}$  elevations (Fig. 5A). Restoration of external  $\text{Ca}^{2+}$  to cooled  
345 cells did not induce a  $[\text{Ca}^{2+}]_{\text{cyt}}$  elevation. However, when these cells were subsequently  
346 warmed to 30 °C and then cooled,  $[\text{Ca}^{2+}]_{\text{cyt}}$  elevations were observed in the majority of cells.  
347 Thus, the generation of cold-induced  $[\text{Ca}^{2+}]_{\text{cyt}}$  elevation depends on the presence of external  
348  $\text{Ca}^{2+}$ , and the  $[\text{Ca}^{2+}]_{\text{cyt}}$  elevation is triggered by the rapid drop in temperature rather than low  
349 absolute temperature itself.

350 *P. tricornutum* lacks cyclic-gated nucleotide channels, which are important for thermal  
351 sensing in plants, although it does possess multiple TRP channels (Verret et al., 2010). The  
352 temperature-sensitive TRPM8 channel in animal cells is responsible for cold induced  $[\text{Ca}^{2+}]_{\text{cyt}}$   
353 elevations and can be activated directly by the plant secondary metabolite, menthol (Yin et al.,  
354 2018). Perfusion of PtR1 cells with 1 mM menthol did not elicit  $[\text{Ca}^{2+}]_{\text{cyt}}$  elevations,  
355 indicating that this ligand is likely specific to the ion channels involved in animal cold  
356 signalling (Fig. 5B). In plant and fungal cells, cold shock induced  $[\text{Ca}^{2+}]_{\text{cyt}}$  elevations have  
357 been studied through the application of dimethyl sulfoxide (DMSO), which is proposed to  
358 mimic cold-induced membrane rigidification (Furuya et al., 2014). DMSO elicited  $[\text{Ca}^{2+}]_{\text{cyt}}$   
359 elevations in a dose-dependent manner in *P. tricornutum*, with 8% and 50% of cells  
360 exhibiting  $\text{Ca}^{2+}$  elevation in response to addition of 1 % and 5% DMSO respectively (n = 24,  
361 25) (Fig.5C-D). Ruthenium red (RR) is a non-selective  $\text{Ca}^{2+}$  channel blocker shown to affect  
362 numerous TRP channels including the cold sensitive TRPA1 channel (Andrade et al., 2008;  
363 Silva et al., 2015; Christensen et al., 2016). RR also inhibits  $[\text{Ca}^{2+}]_{\text{cyt}}$  elevations in *P.*  
364 *tricornutum* induced by the resupply of phosphate to phosphate-limited cells, but does not  
365 inhibit  $[\text{Ca}^{2+}]_{\text{cyt}}$  elevations caused by hypo-osmotic shock (Helliwell et al., 2021; Helliwell et  
366 al., 2021). Pre-treatment of PtR1 cells for 5 mins with 5-10  $\mu\text{M}$  RR did not significantly  
367 reduce the amplitude of cold-induced  $\text{Ca}^{2+}$  elevations (Fig 5E-F). However, RR treated cells  
368 exhibited a significantly slower response time than non-treated control cells (defined as time  
369 from stimulus to the initial elevation above the threshold of  $F/F_0 > 1.5$ ) (Fig. 5G), indicating  
370 that whilst RR does not prevent the cold shock response, it may partially inhibit a component  
371 of the signalling pathway.

372 *P. tricornutum* contains three EukCatA channels, which represent a novel class of voltage-  
373 gated  $\text{Na}^+/\text{Ca}^{2+}$  channel related to single-domain voltage-gated  $\text{Na}^+$  channels in bacteria

374 (BacNav) (Helliwell et al., 2019). As BacNav channels are temperature sensitive (Arrigoni et  
375 al., 2016), we examined whether *P. tricornutum eukcatA1* knockout mutants exhibited an  
376 altered response to cold shock. The percentage of responding cells and the mean maximal  
377 amplitude of the  $[Ca^{2+}]_{cyt}$  elevations did not differ significantly from control PtR1 cells (Fig.  
378 5H-I), indicating that EukCatA1 is not required for cold shock induced  $Ca^{2+}$  signalling.  
379 Further experiments will be needed to determine whether other candidate ion channels, such  
380 as the other EukCatA channels or the diatom TRP channels, contribute to this signalling  
381 response.

382

### 383 **The cold shock response is not required for growth at low temperatures**

384 We next examined whether the cold shock  $Ca^{2+}$  signal was required for *P. tricornutum* cells to  
385 survive following a cold shock. We applied cold shocks in the presence and absence of  
386 external  $Ca^{2+}$  and then monitored their physiology and subsequent growth at 4 °C or 18 °C in  
387 the presence of  $Ca^{2+}$  (Fig 6A). While cells grew significantly more slowly at 4 °C versus 18  
388 °C, there was no significant impact of inhibiting  $Ca^{2+}$  signalling during cold shock on the  
389 ability of cold-shocked cells to grow at either 4 °C or 18 °C (Fig 6B).

390 Growth of *P. tricornutum* at 4 °C promoted the accumulation of the oval morphotype, as  
391 reported previously (De Martino et al., 2011) (Fig 6C). Cells acclimated to low temperatures  
392 may therefore undergo physiological changes that render them less sensitive to rapid cooling.  
393 However, fusiform cells grown at 4 °C for four days still showed a typical cold shock  
394 response with no significant difference in the percentage of cells exhibiting a response (Fig.  
395 6D-E).

396 Taken together, these experiments do not indicate a direct requirement for the  $[Ca^{2+}]_{cyt}$   
397 elevations in protection from rapid cooling alone, as inhibition of the signalling response did  
398 not adversely affect physiology or growth following a cold shock, and the signalling response  
399 was not altered in cells acclimated to low temperatures.

400

### 401 **Interaction between cold and hypo-osmotic shock $Ca^{2+}$ signalling pathways**

402 Diatoms inhabiting inter-tidal regions may regularly experience a cold shock during tidal  
403 cycles (Fig 1), but this is unlikely to represent an isolated stressor. In particular, warming of  
404 shallow tidal pools can greatly increase their salinity due to evaporation (Firth and Williams,  
405 2009), leading to a significant hypo-osmotic shock when the incoming tide reaches the tidal

406 pool. *P. tricornutum* is highly perceptive to hypo-osmotic shock, exhibiting a large transient  
407  $[Ca^{2+}]_{cyt}$  elevation similar to those induced by cold shock (Falciatore et al., 2000; Helliwell et  
408 al., 2021). Since cold and hypo-osmotic shocks are likely to regularly co-occur in intertidal  
409 environments, we examined cellular  $Ca^{2+}$  signalling when these stressors were applied  
410 simultaneously.

411 A relatively mild hypo-osmotic shock (100% ASW to 95% ASW) administered to cells at 25  
412 °C resulted in a single  $[Ca^{2+}]_{cyt}$  elevation, as observed previously (Helliwell et al., 2021) (Fig.  
413 7A). When the same hypo-osmotic shock was applied simultaneously with a cold shock (25  
414 °C to 10 °C), both the amplitude and duration of the  $[Ca^{2+}]_{cyt}$  elevations was substantially  
415 increased, although the number of cells exhibiting  $[Ca^{2+}]_{cyt}$  elevations did not change (Fig.  
416 7A-C). Hypo-osmotic shocks cause an increase in cell volume in *P. tricornutum*, which likely  
417 initiates  $[Ca^{2+}]_{cyt}$  elevations through the activation of mechanosensitive ion channels  
418 (Helliwell et al., 2021). However, cell volume did not increase during cold shock  
419 (Supplemental Fig. S3), indicating that the rapid cooling does not simply elicit  $[Ca^{2+}]_{cyt}$   
420 elevations by mimicking a hypo-osmotic stimulus.

421 A stronger hypo-osmotic shock (100% ASW to 50 % ASW) resulted in a rapid  $[Ca^{2+}]_{cyt}$   
422 elevation which initiated directly after the stimulus was applied (Fig. 7D). In comparison,  
423 application of a cold shock from 34 °C to 8 °C triggered  $[Ca^{2+}]_{cyt}$  elevations that rose less  
424 rapidly and exhibited a longer delay to their initiation (Fig. 7D). Combining both shocks using  
425 perfusion with 50% ASW at 10 °C led to biphasic  $[Ca^{2+}]_{cyt}$  elevations in 71 % of cells (42  
426 cells, three separate experiments) (Fig. 7D). These consisted of a very rapid initial peak in  
427  $[Ca^{2+}]_{cyt}$ , followed by a second peak around 3 s later, which was of greater amplitude than the  
428 first peak in the majority of cells (24 out of 30). The mean maximal amplitude of the  $[Ca^{2+}]_{cyt}$   
429 elevations caused by the three different treatments were all significantly different from each  
430 other, with the cold shock alone causing the lowest and the combined cold- and hypo-osmotic  
431 shock causing the highest  $[Ca^{2+}]_{cyt}$  elevations (Fig. 7E).

432 Taken together,  $[Ca^{2+}]_{cyt}$  elevations induced by hypo-osmotic shock exhibit significant  
433 differences in amplitude and timing in the presence of a simultaneous cold shock. This  
434 indicates that the cold shock stimulus is additive and of sufficient magnitude to influence  
435 cellular  $Ca^{2+}$  signalling during hypo-osmotic stress. We therefore investigated whether  $Ca^{2+}$   
436 signalling during cold shock may influence the short-term survival of *P. tricornutum* under  
437 hypo-osmotic stress.

438

### 439 **Simultaneous cold shock enhances survival during hypo-osmotic shock**

440 Cells were treated with 25% ASW to administer a strong hypo-osmotic shock at control and  
441 low temperatures in the presence or absence of external  $\text{Ca}^{2+}$ . Cell viability was determined  
442 after 3 min by staining with Sytox-Green. Administration of a cold shock alone, either in the  
443 presence or absence of external  $\text{Ca}^{2+}$ , did not reduce cell viability (Fig 8). Application of a  
444 strong hypo-osmotic shock (25% ASW) significantly reduced cell viability, and this effect  
445 was greater following the removal of external  $\text{Ca}^{2+}$ , supporting our previous observations that  
446  $\text{Ca}^{2+}$  signalling is required for osmoregulation and volume control in *P. tricornutum*  
447 (Helliwell et al., 2021). Surprisingly, application of 25% ASW in combination with a cold  
448 shock (4 °C) led to a substantial reduction in cell mortality caused by hypo-osmotic shock  
449 (compared to the control temperature, 21°C). This effect was reduced by inhibiting  $\text{Ca}^{2+}$   
450 signalling, although cell viability remained higher than at control temperature. Our data  
451 therefore indicate that rapid cooling has an important beneficial influence on the survival of *P.*  
452 *tricornutum* cells during a hypo-osmotic shock.

### 453 **Cold shock is associated with $\text{Ca}^{2+}$ -dependent $\text{K}^+$ efflux**

454  $\text{Ca}^{2+}$ -dependent  $\text{K}^+$  efflux plays an essential role in cellular volume control in *P. tricornutum*  
455 during hypo-osmotic shock (Helliwell et al., 2021). We therefore tested whether the  $[\text{Ca}^{2+}]_{\text{cyt}}$   
456 elevations induced by cold shock also resulted in a  $\text{K}^+$  efflux that could influence cellular  
457 osmolarity. We settled a mono-layer of *P. tricornutum* cells onto a microscopy dish and used  
458 a  $\text{K}^+$ -selective microelectrode to measure changes in extracellular  $\text{K}^+$  in the immediate  
459 vicinity of these cells. The cells were perfused with ASW at 25 °C, before rapidly switching  
460 to 12 °C. In each case, the cold shock induced a clear increase in extracellular  $\text{K}^+$  around the  
461 *P. tricornutum* cells (Fig 9A-C). Application of a cold shock in the absence of external  $\text{Ca}^{2+}$   
462 greatly reduced  $\text{K}^+$  efflux from the cells, indicating that the  $\text{K}^+$  efflux is  $\text{Ca}^{2+}$ -dependent. Very  
463 little change in extracellular  $\text{K}^+$  was observed during a cold shock in the absence of cells,  
464 indicating that the performance of the  $\text{K}^+$ -selective microelectrode was not affected by the  
465 change in temperature. We conclude that cold shock induces  $\text{Ca}^{2+}$ -dependent  $\text{K}^+$  efflux in *P.*  
466 *tricornutum* cells, which may contribute to volume regulation during a simultaneous hypo-  
467 osmotic shock.

468



## 469 Discussion

470 This study shows that physiologically significant transient  $[Ca^{2+}]_{cyt}$  elevations are a consistent  
471 response to the rapid cold shocks likely to be experienced by intertidal diatoms. By using a  
472 continuous perfusion system, our study was able to avoid a shear-related  $[Ca^{2+}]_{cyt}$  response,  
473 which may have masked a cold  $[Ca^{2+}]_{cyt}$  response in earlier investigations using *P.*  
474 *tricornutum* expressing aequorin (Falciatore et al., 2000). The cold-induced  $[Ca^{2+}]_{cyt}$   
475 elevations are shown to be specifically involved in sensing the rate of cooling rather than the  
476 absolute temperature. A similar dependence of the amplitude of  $[Ca^{2+}]_{cyt}$  elevations on the rate  
477 of cooling has been observed in *Arabidopsis*, which showed  $[Ca^{2+}]_{cyt}$  elevations at cooling  
478 rates down to  $0.05\text{ }^{\circ}\text{C s}^{-1}$ , (Plieth et al., 1999) indicating greater sensitivity of *Arabidopsis* to  
479 slower cooling rates. *P. tricornutum* and *T. pseudonana* did not show a  $Ca^{2+}$  signalling  
480 response to rapid warming, suggesting that the  $Ca^{2+}$  signalling pathways of animals and plants  
481 in response to elevated temperatures are not conserved in diatoms. Diatoms therefore likely  
482 use alternative cellular mechanisms for thermosensation in response to rapid heat shock,  
483 although as only short-term temperature increases were evaluated in our study, we cannot rule  
484 out a potential role for  $Ca^{2+}$  signalling in response to longer term temperature increases.

485 Cold shock-induced  $[Ca^{2+}]_{cyt}$  elevations in *P. tricornutum* do not play an obvious role in  
486 acclimation to low temperatures. We found no longer-term growth effects of experimentally  
487 blocking the cold shock  $Ca^{2+}$  signal. Cold signalling in *P. tricornutum* therefore differs from  
488 plants and insects (Knight and Knight, 2012; Teets et al., 2013), in which the  $[Ca^{2+}]_{cyt}$   
489 elevations play a direct role in acclimation to lower temperatures. The  $[Ca^{2+}]_{cyt}$  response in *P.*  
490 *tricornutum* is specifically induced by rapid cooling, which points to a potential role in short-  
491 term regulation of cellular processes rather than longer term acclimation to a change in  
492 temperature. Of particular interest is the interaction between cold shock and osmotic shock,  
493 since inter-tidal organisms are often likely to experience these stresses simultaneously, during  
494 an incoming tide or rain precipitation (Lewin and Guillard, 1963; Kirst, 1990). Given the  
495 nature of the osmotic and cold shock  $Ca^{2+}$  signals identified in *P. tricornutum*, it is most likely  
496 that they involve distinct sensory pathways, as evidenced by their additive nature and the  
497 appearance of a biphasic  $[Ca^{2+}]_{cyt}$  elevation when cells were treated with simultaneous cold  
498 and osmotic shocks. Whether these distinct responses represent  $Ca^{2+}$  entry through different  
499  $Ca^{2+}$  channels or are due to sequential activation of the same  $Ca^{2+}$  channel by different stimuli  
500 with little or no refractory period remains to be determined, although it is worthy of note that  
501 both the osmotic (Helliwell et al., 2021) and the cold-induced  $Ca^{2+}$  signals initiate at the cell

502 apices (Fig 2B). Cold and osmotic  $\text{Ca}^{2+}$  signals also both require the presence of external  
503  $\text{Ca}^{2+}$ , indicating a shared requirement for plasma membrane  $\text{Ca}^{2+}$  channels, at least in the  
504 initiation of the  $[\text{Ca}^{2+}]_{\text{cyt}}$  elevation.

505 The protective effect of cold shock on survival of *P. tricornutum* in response to severe  
506 osmotic shock may arise directly from cooperative  $\text{Ca}^{2+}$  signalling (Supplemental Fig. S4).  
507 The hypo-osmotic shock induced  $[\text{Ca}^{2+}]_{\text{cyt}}$  elevations lead to rapid efflux of  $\text{K}^+$  in *P.*  
508 *tricornutum*, which restricts cell volume increase and prevents bursting (Helliwell et al.,  
509 2021). The results here strongly suggest that cold-induced  $[\text{Ca}^{2+}]_{\text{cyt}}$  elevations may also act  
510 directly to trigger  $\text{K}^+$  efflux from the cytosol, for example through the activation of  $\text{Ca}^{2+}$ -  
511 dependent  $\text{K}^+$  channels. Whether the rapid loss of  $\text{K}^+$  plays a physiological role in acclimation  
512 to low temperature is unclear, but it would clearly serve to lower the osmolarity of the cell.  
513 Given the frequent co-occurrence of cold and hypo-osmotic shocks, the cold-induced  $[\text{Ca}^{2+}]_{\text{cyt}}$   
514 elevations may therefore function primarily to support osmoregulation. Rapid cooling does  
515 not appear to adversely harm the cell when  $\text{Ca}^{2+}$  signalling is inhibited, whereas a severe  
516 hypo-osmotic shock will lead to cell bursting within seconds if cell volume is not controlled  
517 (Helliwell et al., 2021).

518 Osmoregulation in response to hypo-osmotic stress in diatoms (and most other eukaryotes) is  
519 most likely initiated by activation of mechanosensitive channels due to the increase in cell  
520 volume (Helliwell et al., 2021). Mechanosensitive channels only activate when the membrane  
521 is under tension, i.e. when swelling has already occurred, and cell viability is therefore under  
522 immediate threat if rapid osmoregulation cannot be achieved. The  $\text{K}^+$  efflux in response to a  
523 cold shock would allow the cell to reduce its osmolarity even if this critical increase in  
524 membrane tension is not perceived. By associating  $\text{K}^+$  efflux with an additional stimulus that  
525 commonly co-occurs with hypo-osmotic shock, diatoms can augment the osmoregulatory  
526 response and help prevent cell swelling to critical levels. Consistent with this hypothesis,  
527 cold-induced  $[\text{Ca}^{2+}]_{\text{cyt}}$  elevations were only associated with very rapid cooling. A more  
528 gradual exposure to hypo-osmotic stress conveys a much lower risk of cell bursting, reducing  
529 the need to augment the osmoregulatory response.

530 We should also consider that low temperature may have a direct effect on reducing mortality  
531 during hypo-osmotic stress that is independent of the signalling component, for example by  
532 increasing cell wall rigidity. However, the protective effect of cold shock in the absence of  
533  $\text{Ca}^{2+}$  was small compared to the much greater reduction in mortality in the presence of  
534 external  $\text{Ca}^{2+}$ . We were unable to identify pharmacological inhibitors to selectively inhibit

535 either osmotic or cold associated  $\text{Ca}^{2+}$  signalling and the removal of external  $\text{Ca}^{2+}$  completely  
536 inhibited both signalling pathways. Dissecting the individual contributions of these signalling  
537 pathways to cell survival during simultaneous shocks is therefore not currently easily  
538 achieved. Selective inactivation of the underlying molecular mechanisms through genetic  
539 approaches will most likely be required to fully understand the nature of the cross-talk  
540 between the signalling pathways.

541 Cellular responses to stressors are commonly examined in isolation in the laboratory in order  
542 to simplify the elucidation of the signalling pathways responsible. However, organisms often  
543 have to respond to inputs from multiple stimuli simultaneously in their natural environment,  
544 leading to cross-talk between signalling pathways. Cross-talk in cell signalling can occur  
545 when two distinct stimuli trigger a shared cellular response that confers tolerance to both  
546 stressors. This may involve activation of a common receptor or activation of independent  
547 receptors that converge on a specific node in the signalling pathway (Knight and Knight,  
548 2001). Cross-talk with temperature sensing is likely to have evolved when another stress  
549 occurs simultaneously with temperature or with a predictable temporal link (i.e. one stimulus  
550 consistently precedes the other) (Sinclair et al., 2013). In the case of the inter-tidal zone, many  
551 environmental parameters will exhibit a degree of co-variance associated with tidal immersion  
552 and emersion. It seems likely that organisms inhabiting these environments have developed  
553 mechanisms of cross-talk in their pathways of environmental perception that enable them  
554 optimise their physiological responses.

555 There are multiple examples of cross-talk between temperature and osmotic stress signalling  
556 pathways in other eukaryotes. In plants, freezing temperatures can lead to cellular water loss  
557 due to external ice formation and many of the genes within the cold-inducible COR regulon  
558 are also inducible by drought (Boyce et al., 2003). The cold-responsive CBF/DREB1 and  
559 drought-responsive DREB2 transcription factors both bind to a common promoter element  
560 (DRE), leading to convergence of the cold and drought signalling pathways (Boyce et al.,  
561 2003). Overexpression of the cold-responsive DREB1A transcription factor in *Arabidopsis*  
562 resulted in enhanced tolerance to both freezing and drought stress (Liu et al., 1998). In  
563 addition, *Arabidopsis* plants treated with the phytohormone abscisic acid, which plays a  
564 primary role in drought tolerance, also show enhanced freezing tolerance (Mantyla et al.,  
565 1995). Cross-talk between temperature and osmotic stress signalling pathways have also been  
566 documented in yeast. *Saccharomyces cerevisiae* exhibits a high osmolarity (HOG) response to  
567 hyper-osmotic stress that results in increased production of the compatible solute, glycerol.

568 The HOG response is mediated by a mitogen-activated protein kinase (MAPK) pathway that  
569 can also be activated by other stimuli including both cold and heat shocks. Heat shock  
570 activates the HOG pathway indirectly by stimulating loss of glycerol, leading to hyper-  
571 osmotic stress (Winkler et al., 2002; Dunayevich et al., 2018).

572 Our results indicate that cross-talk between  $\text{Ca}^{2+}$ -mediated cellular signalling mechanisms is  
573 an important consideration in the response of marine organisms to multiple stressors. Whilst  
574 our results are discussed primarily in the context of the inter-tidal zone where rapid  
575 substantial changes in temperature are a regular occurrence, the conserved nature of cold-  
576 induced  $\text{Ca}^{2+}$  signalling in *T. pseudonana* suggests that this pathway may be important more  
577 widely in diatom ecology. The cold-induced  $[\text{Ca}^{2+}]_{\text{cyt}}$  elevations in *T. pseudonana* exhibit  
578 different characteristics from *P. tricornutum* that may reflect differences in their physiological  
579 response. Planktonic diatoms will undoubtedly encounter significant fluctuations in  
580 temperature and salinity in near-shore and estuarine environments or when they are mixed  
581 through the thermocline, although the magnitude and rate of the temperature changes are  
582 likely to be lower. Diatoms inhabiting sea ice environments may also experience rapid  
583 changes in temperature and salinity e.g. during flushing of hyper-saline brine channels with  
584 melt water (Mock and Junge, 2007). Future elucidation of the mechanisms of cross talk in  
585 these signalling pathways will allow us to understand how diatoms successfully integrate  
586 inputs from multiple environmental stimuli, which has likely played a major role in their  
587 success in diverse and highly dynamic environmental regimes.

588 **Acknowledgements:**

589 The work was supported by an ERC Advanced Grant to CB (ERC-ADG-670390) and a  
590 NERC award to GLW (NE/V013343/1).

591

592 **Author contributions**

593 CB, FK and GLW conceived the study. FK performed the majority of the experimental  
594 analyses, including all imaging experiments. KEH contributed to measurements of osmotic  
595 stress. AC performed  $K^+$  microelectrode measurements. HPW and NM performed the  
596 environmental monitoring. TM, AH and TG contributed to the transformation of *T.*  
597 *pseudonana* with R-GECO1. GLW, CB and FK analysed the data and wrote the manuscript.

598

599 **References**

- 600 **Alverson AJ, Beszteri B, Julius ML, Theriot EC** (2011) The model marine diatom  
601 *Thalassiosira pseudonana* likely descended from a freshwater ancestor in the genus  
602 Cyclotella. *BMC Evol Biol* **11**: 125
- 603 **Anderson SI, Rynearson TA** (2020) Variability approaching the thermal limits can drive  
604 diatom community dynamics. *Limnology and Oceanography* **65**: 1961-1973
- 605 **Andrade EL, Luiz AP, Ferreira J, Calixto JB** (2008) Pronociceptive response elicited by  
606 TRPA1 receptor activation in mice. *Neuroscience* **152**: 511-520
- 607 **Arrigoni C, Rohaim A, Shaya D, Findeisen F, Stein RA, Nurva SR, Mishra S,  
608 McHaourab HS, Minor DL, Jr.** (2016) Unfolding of a temperature-sensitive domain  
609 controls voltage-gated channel activation. *Cell* **164**: 922-936
- 610 **Baker KG, Geider RJ** (2021) Phytoplankton mortality in a changing thermal seascape. *Glob*  
611 *Chang Biol*
- 612 **Boyce JM, Knight H, Deyholos M, Openshaw MR, Galbraith DW, Warren G, Knight  
613 MR** (2003) The *sfr6* mutant of *Arabidopsis* is defective in transcriptional activation  
614 via CBF/DREB1 and DREB2 and shows sensitivity to osmotic stress. *Plant J* **34**: 395-  
615 406
- 616 **Christensen AP, Akyuz N, Corey DP** (2016) The outer pore and selectivity filter of TRPA1.  
617 *PLoS One* **11**: e0166167
- 618 **Clapham DE, Miller C** (2011) A thermodynamic framework for understanding temperature  
619 sensing by transient receptor potential (TRP) channels. *Proc Natl Acad Sci U S A* **108**:  
620 19492-19497
- 621 **Cui Y, Lu S, Li Z, Cheng J, Hu P, Zhu T, Wang X, Jin M, Wang X, Li L, Huang S, Zou  
622 B, Hua J** (2020) Cyclic nucleotide-gated ion channels 14 and 16 promote tolerance to  
623 heat and chilling in rice. *Plant Physiol* **183**: 1794-1808
- 624 **De Martino A, Bartual A, Willis A, Meichenin A, Villazan B, Maheswari U, Bowler C**  
625 (2011) Physiological and molecular evidence that environmental changes elicit  
626 morphological interconversion in the model diatom *Phaeodactylum tricornutum*.  
627 *Protist* **162**: 462-481
- 628 **De Martino A, Meichenin A, Shi J, Pan KH, Bowler C** (2007) Genetic and phenotypic  
629 characterization of *Phaeodactylum tricornutum* (Bacillariophyceae) accessions.  
630 *Journal of Phycology* **43**: 992-1009
- 631 **Dunayevich P, Baltanas R, Clemente JA, Couto A, Sapochnik D, Vasen G, Colman-  
632 Lerner A** (2018) Heat-stress triggers MAPK crosstalk to turn on the hyperosmotic  
633 response pathway. *Sci Rep* **8**: 15168
- 634 **Falciatore A, d'Alcala MR, Croot P, Bowler C** (2000) Perception of environmental signal  
635 by a marine diatom. *Science* **288**: 2363-2366
- 636 **Firth LB, Williams GA** (2009) The influence of multiple environmental stressors on the  
637 limpet *Cellana toreuma* during the summer monsoon season in Hong Kong. *Journal of*  
638 *Experimental Marine Biology and Ecology* **375**: 70-75
- 639 **Furuya T, Matsuoka D, Nanmori T** (2014) Membrane rigidification functions upstream of  
640 the MEKK1-MKK2-MPK4 cascade during cold acclimation in *Arabidopsis thaliana*.  
641 *FEBS Lett* **588**: 2025-2030
- 642 **Gattuso JP, Magnan A, Bille R, Cheung WWL, Howes EL, Joos F, Allemand D, Bopp L,  
643 Cooley SR, Eakin CM, Hoegh-Guldberg O, Kelly RP, Portner HO, Rogers AD,  
644 Baxter JM, Laffoley D, Osborn D, Rankovic A, Rochette J, Sumaila UR, Treyer  
645 S, Turley C** (2015) Contrasting futures for ocean and society from different  
646 anthropogenic CO<sub>2</sub> emissions scenarios. *Science* **349**
- 647 **Gruber N, Boyd PW, Frolicher TL, Vogt M** (2021) Biogeochemical extremes and  
648 compound events in the ocean. *Nature* **600**: 395-407

649 **Guillard RL** (1975) Culture of phytoplankton for feeding marine invertebrates. Culture of  
650 Marine Invertebrate Animals: 29-60

651 **Harley CDG, Hughes AR, Hultgren KM, Miner BG, Sorte CJB, Thornber CS,**  
652 **Rodriguez LF, Tomanek L, Williams SL** (2006) The impacts of climate change in  
653 coastal marine systems. *Ecology Letters* **9**: 228-241

654 **Helliwell KE, Chrachri A, Koester JA, Wharam S, Verret F, Taylor AR, Wheeler GL,**  
655 **Brownlee C** (2019) Alternative mechanisms for fast  $\text{Na}^+/\text{Ca}^{2+}$  signaling in eukaryotes  
656 via a novel class of single-domain voltage-gated channels. *Curr Biol* **29**: 1503-1511  
657 e1506

658 **Helliwell KE, Harrison EL, Christie-Oleza JA, Rees AP, Kleiner FH, Gaikwad T,**  
659 **Downe J, Aguilo-Ferretjans MM, Al-Moosawi L, Brownlee C, Wheeler GL**  
660 (2021) A Novel  $\text{Ca}^{2+}$  signaling pathway coordinates environmental phosphorus  
661 sensing and nitrogen metabolism in marine diatoms. *Curr Biol* **31**: 978-989 e974

662 **Helliwell KE, Kleiner FH, Hardstaff H, Chrachri A, Gaikwad T, Salmon D, Smirnov N,**  
663 **Wheeler GL, Brownlee C** (2021) Spatiotemporal patterns of intracellular  $\text{Ca}^{2+}$   
664 signalling govern hypo-osmotic stress resilience in marine diatoms. *New Phytol* **230**:  
665 155-170

666 **J C Lewin a, Guillard RRL** (1963) Diatoms. *Annual Review of Microbiology* **17**: 373-414

667 **Javaheri N, Dries R, Burson A, Stal LJ, Sloop PMA, Kaandorp JA** (2015) Temperature  
668 affects the silicate morphology in a diatom. *Scientific Reports* **5**: 11652 .

669 **Kirst GO** (1990) Salinity tolerance of eukaryotic marine-algae. *Annual Review of Plant*  
670 *Physiology and Plant Molecular Biology* **41**: 21-53

671 **Knight H, Knight MR** (2001) Abiotic stress signalling pathways: specificity and cross-talk.  
672 *Trends Plant Sci* **6**: 262-267

673 **Knight H, Trewavas AJ, Knight MR** (1996) Cold calcium signaling in *Arabidopsis* involves  
674 two cellular pools and a change in calcium signature after acclimation. *Plant Cell* **8**:  
675 489-503

676 **Knight MR, Knight H** (2012) Low-temperature perception leading to gene expression and  
677 cold tolerance in higher plants. *New Phytol* **195**: 737-751

678 **Lenzoni G, Knight MR** (2019) Increases in absolute temperature stimulate free calcium  
679 concentration elevations in the chloroplast. *Plant Cell Physiol* **60**: 538-548

680 **Lewin JC, Guillard RRL** (1963) Diatoms. *Annual Review of Microbiology* **17**: 373-414

681 **Liang Y, Koester JA, Liefer JD, Irwin AJ, Finkel ZV** (2019) Molecular mechanisms of  
682 temperature acclimation and adaptation in marine diatoms. *ISME J* **13**: 2415-2425

683 **Liu Q, Ding Y, Shi Y, Ma L, Wang Y, Song C, Wilkins KA, Davies JM, Knight H,**  
684 **Knight MR, Gong Z, Guo Y, Yang S** (2021) The calcium transporter ANNEXIN1  
685 mediates cold-induced calcium signaling and freezing tolerance in plants. *EMBO J* **40**:  
686 e104559

687 **Liu Q, Kasuga M, Sakuma Y, Abe H, Miura S, Yamaguchi-Shinozaki K, Shinozaki K**  
688 (1998) Two transcription factors, DREB1 and DREB2, with an EREBP/AP2 DNA  
689 binding domain separate two cellular signal transduction pathways in drought- and  
690 low-temperature-responsive gene expression, respectively, in *Arabidopsis*. *Plant Cell*  
691 **10**: 1391-1406

692 **Ma Y, Dai X, Xu Y, Luo W, Zheng X, Zeng D, Pan Y, Lin X, Liu H, Zhang D, Xiao J,**  
693 **Guo X, Xu S, Niu Y, Jin J, Zhang H, Xu X, Li L, Wang W, Qian Q, Ge S, Chong**  
694 **K** (2015) COL1D1 confers chilling tolerance in rice. *Cell* **160**: 1209-1221

695 **Malviya S, Scalco E, Audic S, Vincent F, Veluchamy A, Poulain J, Wincker P, Iudicone**  
696 **D, de Vargas C, Bittner L, Zingone A, Bowler C** (2016) Insights into global diatom  
697 distribution and diversity in the world's ocean. *Proc Natl Acad Sci U S A* **113**: E1516-  
698 1525

- 699 **Mantyla E, Lang V, Palva ET** (1995) Role of abscisic acid in drought-induced freezing  
700 tolerance, cold acclimation, and accumulation of LT178 and RAB18 proteins in  
701 *Arabidopsis thaliana*. *Plant Physiol* **107**: 141-148
- 702 **Mock T, Junge K** (2007) PSYCHROPHILIC DIATOMS: Mechanisms for survival in  
703 freeze–thaw cycles. In J Seckbach, ed, *Algae and Cyanobacteria in Extreme*  
704 *Environments*. Springer, pp 343-364
- 705 **Montagnes DJS, Franklin DJ** (2001) Effect of temperature on diatom volume, growth rate,  
706 and carbon and nitrogen content: Reconsidering some paradigms. *Limnology and*  
707 *Oceanography* **46**: 2008-2018
- 708 **Ohkura M, Sasaki T, Sadakari J, Gengyo-Ando K, Kagawa-Nagamura Y, Kobayashi C,**  
709 **Ikegaya Y, Nakai J** (2012) Genetically encoded green fluorescent Ca<sup>2+</sup> indicators  
710 with improved detectability for neuronal Ca<sup>2+</sup> signals. *PLoS One* **7**: e51286
- 711 **Plieth C, Hansen UP, Knight H, Knight MR** (1999) Temperature sensing by plants: the  
712 primary characteristics of signal perception and calcium response. *Plant J* **18**: 491-497
- 713 **Pokorna J, Schwarzerova K, Zelenkova S, Petrasek J, Janotova I, Capkova V, Opatrny**  
714 **Z** (2004) Sites of actin filament initiation and reorganization in cold-treated tobacco  
715 cells. *Plant Cell and Environment* **27**: 641-653
- 716 **Saidi Y, Finka A, Muriset M, Bromberg Z, Weiss YG, Maathuis FJ, Goloubinoff P**  
717 (2009) The heat shock response in moss plants is regulated by specific calcium-  
718 permeable channels in the plasma membrane. *Plant Cell* **21**: 2829-2843
- 719 **Schaum CE, Buckling A, Smirnoff N, Studholme DJ, Yvon-Durocher G** (2018)  
720 Environmental fluctuations accelerate molecular evolution of thermal tolerance in a  
721 marine diatom. *Nat Commun* **9**: 1719
- 722 **Sengupta P, Garrity P** (2013) Sensing temperature. *Curr Biol* **23**: R304-307
- 723 **Silva DF, de Almeida MM, Chaves CG, Braz AL, Gomes MA, Pinho-da-Silva L,**  
724 **Pesquero JL, Andrade VA, Leite Mde F, de Albuquerque JG, Araujo IG, Nunes**  
725 **XP, Barbosa-Filho JM, Cruz Jdos S, Correia Nde A, de Medeiros IA** (2015)  
726 TRPM8 channel activation induced by monoterpenoid rotundifolone underlies  
727 mesenteric artery relaxation. *PLoS One* **10**: e0143171
- 728 **Sinclair BJ, Ferguson LV, Salehipour-shirazi G, MacMillan HA** (2013) Cross-tolerance  
729 and cross-talk in the cold: relating low temperatures to desiccation and immune stress  
730 in insects. *Integr Comp Biol* **53**: 545-556
- 731 **Smale DA, Wernberg T, Oliver ECJ, Thomsen M, Harvey BP, Straub SC, Burrows MT,**  
732 **Alexander LV, Benthuisen JA, Donat MG, Feng M, Hobday AJ, Holbrook NJ,**  
733 **Perkins-Kirkpatrick SE, Scannell HA, Sen Gupta A, Payne BL, Moore PJ** (2019)  
734 Marine heatwaves threaten global biodiversity and the provision of ecosystem  
735 services. *Nature Climate Change* **9**: 306-+
- 736 **Souffreau C, Vanormelingen P, Verleyen E, Sabbe K, Vyverman W** (2010) Tolerance of  
737 benthic diatoms from temperate aquatic and terrestrial habitats to experimental  
738 desiccation and temperature stress. *Phycologia* **49**: 309-324
- 739 **Svensson F, Norberg J, Snoeijs P** (2014) Diatom cell size, coloniality and motility: trade-  
740 offs between temperature, salinity and nutrient supply with climate change. *Plos One* **9**
- 741 **Tahtiharju S, Sangwan V, Monroy AF, Dhindsa RS, Borg M** (1997) The induction of kin  
742 genes in cold-acclimating *Arabidopsis thaliana*. Evidence of a role for calcium. *Planta*  
743 **203**: 442-447
- 744 **Teets NM, Yi SX, Lee RE, Jr., Denlinger DL** (2013) Calcium signaling mediates cold  
745 sensing in insect tissues. *Proc Natl Acad Sci U S A* **110**: 9154-9159
- 746 **Vardi A, Formiggini F, Casotti R, De Martino A, Ribalet F, Miralto A, Bowler C** (2006)  
747 A stress surveillance system based on calcium and nitric oxide in marine diatoms. *Plos*  
748 *Biology* **4**: 411-419



749 **Verret F, Wheeler G, Taylor AR, Farnham G, Brownlee C** (2010) Calcium channels in  
750 photosynthetic eukaryotes: implications for evolution of calcium-based signalling.  
751 *New Phytol* **187**: 23-43

752 **Winkler A, Arkind C, Mattison CP, Burkholder A, Knoche K, Ota I** (2002) Heat stress  
753 activates the yeast high-osmolarity glycerol mitogen-activated protein kinase pathway,  
754 and protein tyrosine phosphatases are essential under heat stress. *Eukaryot Cell* **1**:  
755 163-173

756 **Xu H, Ramsey IS, Kotecha SA, Moran MM, Chong JA, Lawson D, Ge P, Lilly J, Silos-**  
757 **Santiago I, Xie Y, DiStefano PS, Curtis R, Clapham DE** (2002) TRPV3 is a  
758 calcium-permeable temperature-sensitive cation channel. *Nature* **418**: 181-186

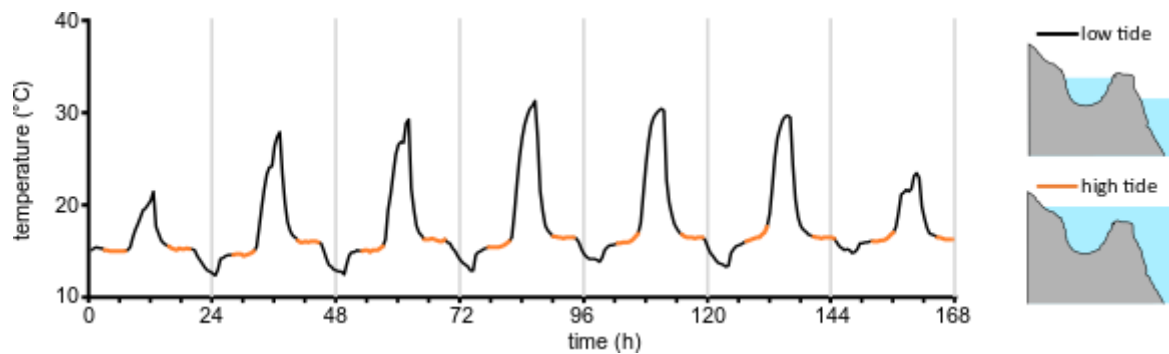
759 **Yin Y, Wu M, Zubcevic L, Borschel WF, Lander GC, Lee SY** (2018) Structure of the  
760 cold- and menthol-sensing ion channel TRPM8. *Science* **359**: 237-241

761 **Zhao Y, Araki S, Wu J, Teramoto T, Chang YF, Nakano M, Abdelfattah AS, Fujiwara**  
762 **M, Ishihara T, Nagai T, Campbell RE** (2011) An expanded palette of genetically  
763 encoded Ca<sup>2+</sup> indicators. *Science* **333**: 1888-1891

764

765 **Figures**

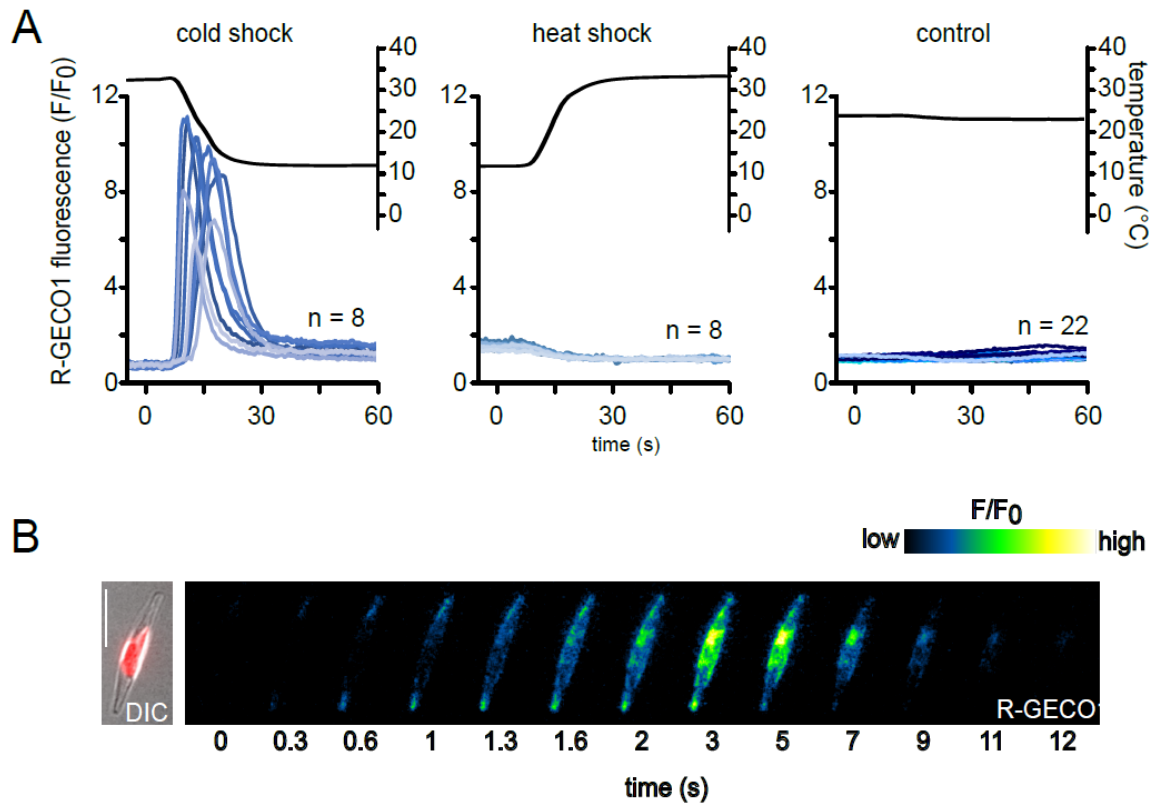
766



767

768

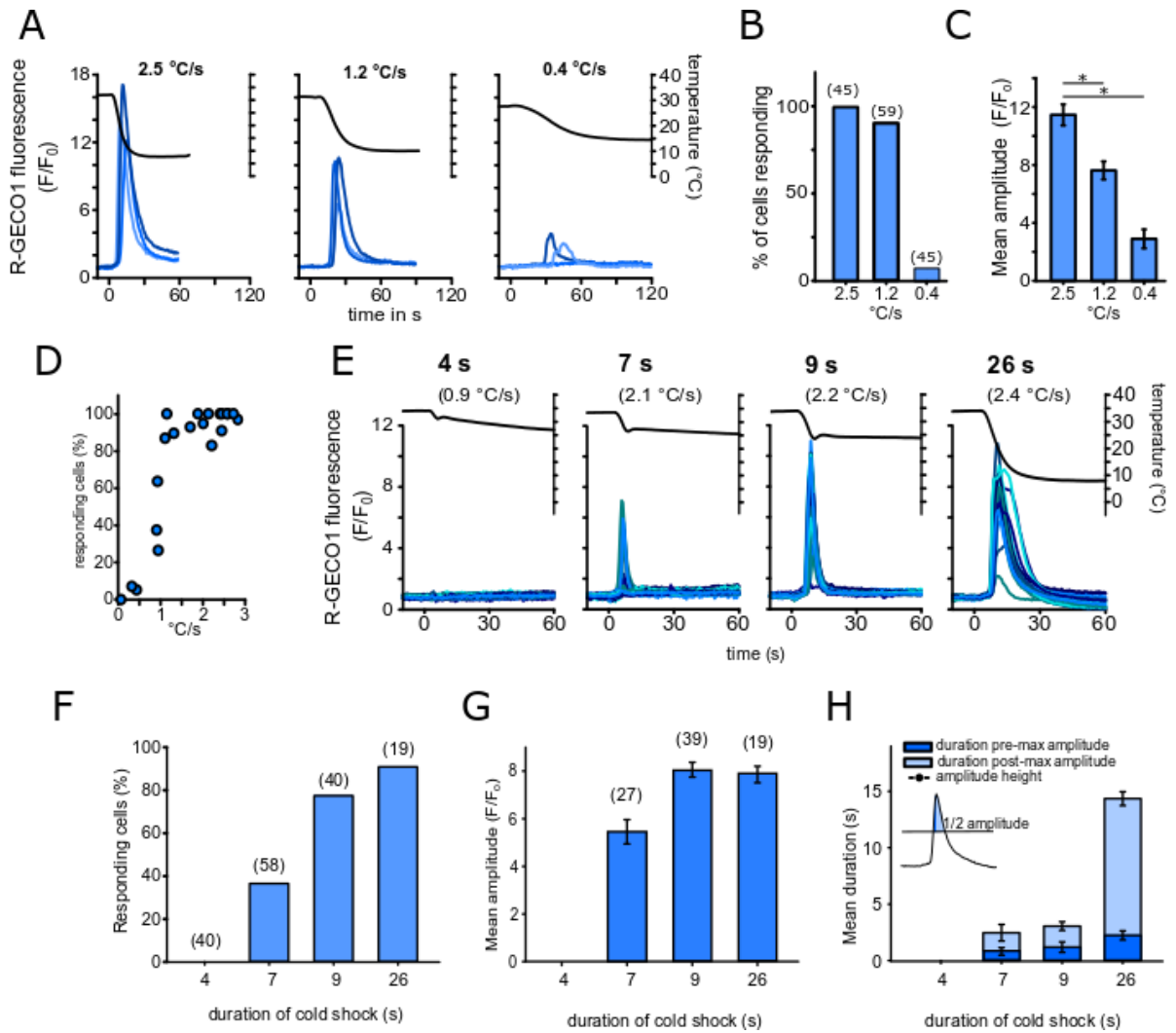
769 **Figure 1: Temperature fluctuations in the inter-tidal zone.** An example of temperature  
770 fluctuations measured in a temperate coastal rock pool (Looe, Cornwall, UK) over the course  
771 of seven days in summer (01/07/2019-07/07/2019). Orange colour indicates periods at which  
772 the pool was immersed by the high tide (approx. duration of immersion 5 h). Significant  
773 excursions from the sea temperature occur when the rock pool is isolated from the bulk  
774 seawater at low tide (black traces). Rapid cooling (30 °C to 15 °C) occurs when the incoming  
775 tide reaches the pool.



776

777

778 **Figure 2: *P. tricornutum* exhibits cytosolic Ca<sup>2+</sup> ([Ca<sup>2+</sup>]<sub>cyt</sub>) elevations in response to rapid**  
 779 **cooling. A)** Eight representative fluorescence ratio traces (F/F<sub>0</sub>, blue lines) of *P. tricornutum*  
 780 cells expressing R-GECO1 representing changes in cytosolic Ca<sup>2+</sup>. Cells were perfused with  
 781 ASW of different temperatures to cause rapid temperature shifts (black line). Cold shock 30  
 782 °C to 12 °C, heat shock 12 °C to 30 °C or control 22 °C to 22 °C. **B)** False colour images of a  
 783 PtR1 cell exhibiting a [Ca<sup>2+</sup>]<sub>cyt</sub> elevation in response to cold shock. The temperature decrease  
 784 begins at t = 0 s. Note that the [Ca<sup>2+</sup>]<sub>cyt</sub> elevations initiate at the tips of the cell and spread  
 785 towards the central region. Left panel indicates a DIC image overlaid with chlorophyll  
 786 autofluorescence. Bar represents 10 μm.

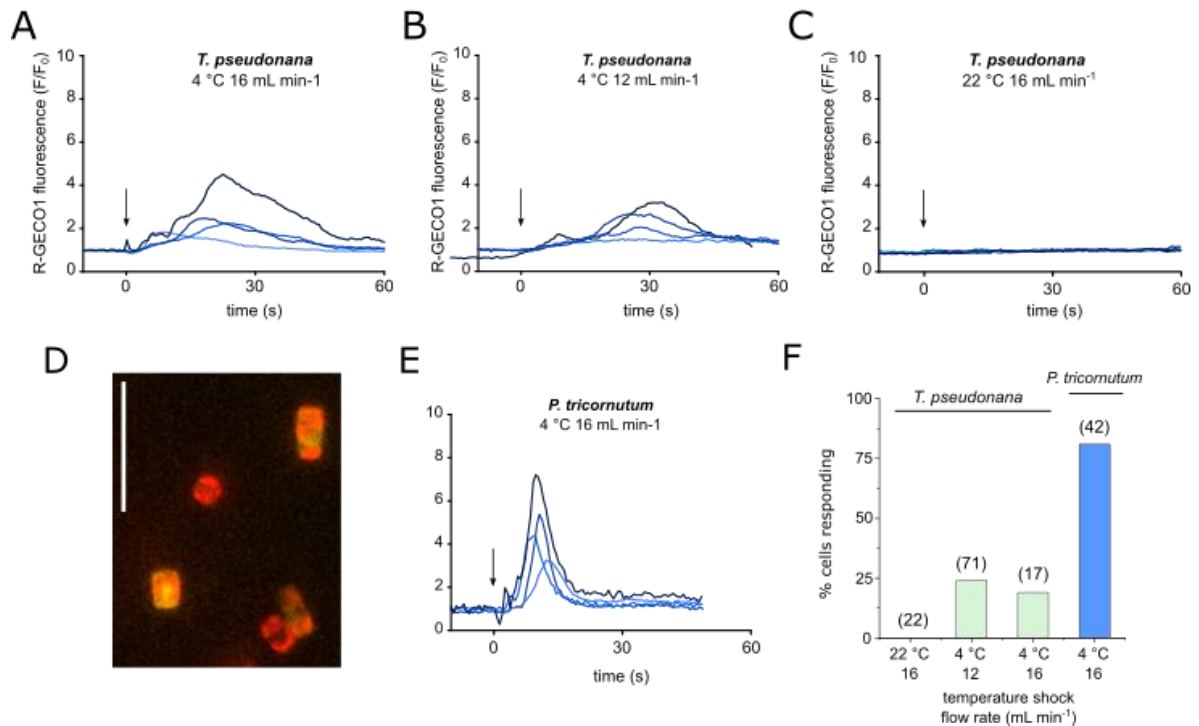


787

788 **Figure 3: The cold shock  $Ca^{2+}$  response depends on the rate of change of temperature.**

789 **A)** R-GECO1 fluorescence in *P. tricornutum* in response to cold shock administered at  
 790 different cooling rates. As cooling rates were non-linear the maximal cooling rate for each  
 791 treatment was calculated for comparisons. Three representative traces are shown. **B)** The  
 792 percentage of cells exhibiting a  $[Ca^{2+}]_{cyt}$  elevation ( $F/F_0 > 1.5$ ) at different cooling rates. Total  
 793 number of cells examined are shown in parentheses, from a minimum of two separate  
 794 experimental treatments. **C)** Mean maximal amplitude of  $[Ca^{2+}]_{cyt}$  elevations from responsive  
 795 cells in (B). \* indicates a significant difference (One way ANOVA on Ranks  $P > 0.001$ ,  
 796 Dunn's post-hoc test  $P > 0.001$ ).  $n = 31, 30$  and  $3$  for  $2.5, 1.2$  and  $0.4 \text{ } ^\circ\text{C s}^{-1}$  respectively. Error  
 797 bars = SE. **D)** Percentage of cells responding to cold shock with a  $[Ca^{2+}]_{cyt}$  elevation across a  
 798 broader range of maximum cooling rates. The data represent 21 independent experiments,  
 799 with a mean of 38 cells examined for each data point (minimum 12, maximum 123 cells). **E)**  
 800  $[Ca^{2+}]_{cyt}$  elevations in response to different durations of cooling applied with a constant flow  
 801 rate ( $16 \text{ mL min}^{-1}$ ). 20 representative traces from PtR1 cells are shown, with greater  $[Ca^{2+}]_{cyt}$   
 802 elevations observed under increasing durations of cold shock. The maximum rate of

803 temperature decrease ( $\Delta T \text{ s}^{-1}$ ) is shown in parantheses. Data for 4, 7, 9 and 26 s of cold shock  
804 duration were compiled from 2, 3, 2 and 1 individual experiments, respectively. **F)** The  
805 percentage of cells exhibiting a  $[\text{Ca}^{2+}]_{\text{cyt}}$  elevation in response to cold shock for the  
806 experiment described in (E). **G)** Mean maximal amplitude of  $[\text{Ca}^{2+}]_{\text{cyt}}$  elevations in response to  
807 cold shock for the responding cells shown in (F). **H)** Duration of  $[\text{Ca}^{2+}]_{\text{cyt}}$  elevations (shown  
808 as full width at half maximum amplitude) in relation of the duration of cold stimulus. The  
809 duration of  $[\text{Ca}^{2+}]_{\text{cyt}}$  elevations is greatest at the 26 s cold shock. The duration is divided into a  
810 pre- and post-maximal amplitude component to show that the post-maximal amplitude (tail)  
811 components of the  $[\text{Ca}^{2+}]_{\text{cyt}}$  elevation is greatly extended under the 26 s cold shock.



812

813 **Figure 4: *Thalassiosira pseudonana* also shows cold-induced  $[Ca^{2+}]_{cyt}$  elevations. A)**

814 Fluorescence ratio of *T. pseudonana* cells expressing cytosolic R-GECO1 in response to a

815 cold shock (from 30 to 10 °C). For these experiments the temperature in the dish was not

816 monitored, so perfusion flow rate is shown to indicate rate of cold shock. Arrow indicates

817 onset of cold stimulus. Four representative traces are shown. B) As in (A) but at a slower flow

818 rate. C) Treatment control using perfusion of ASW at room temperature. D) Fluorescence

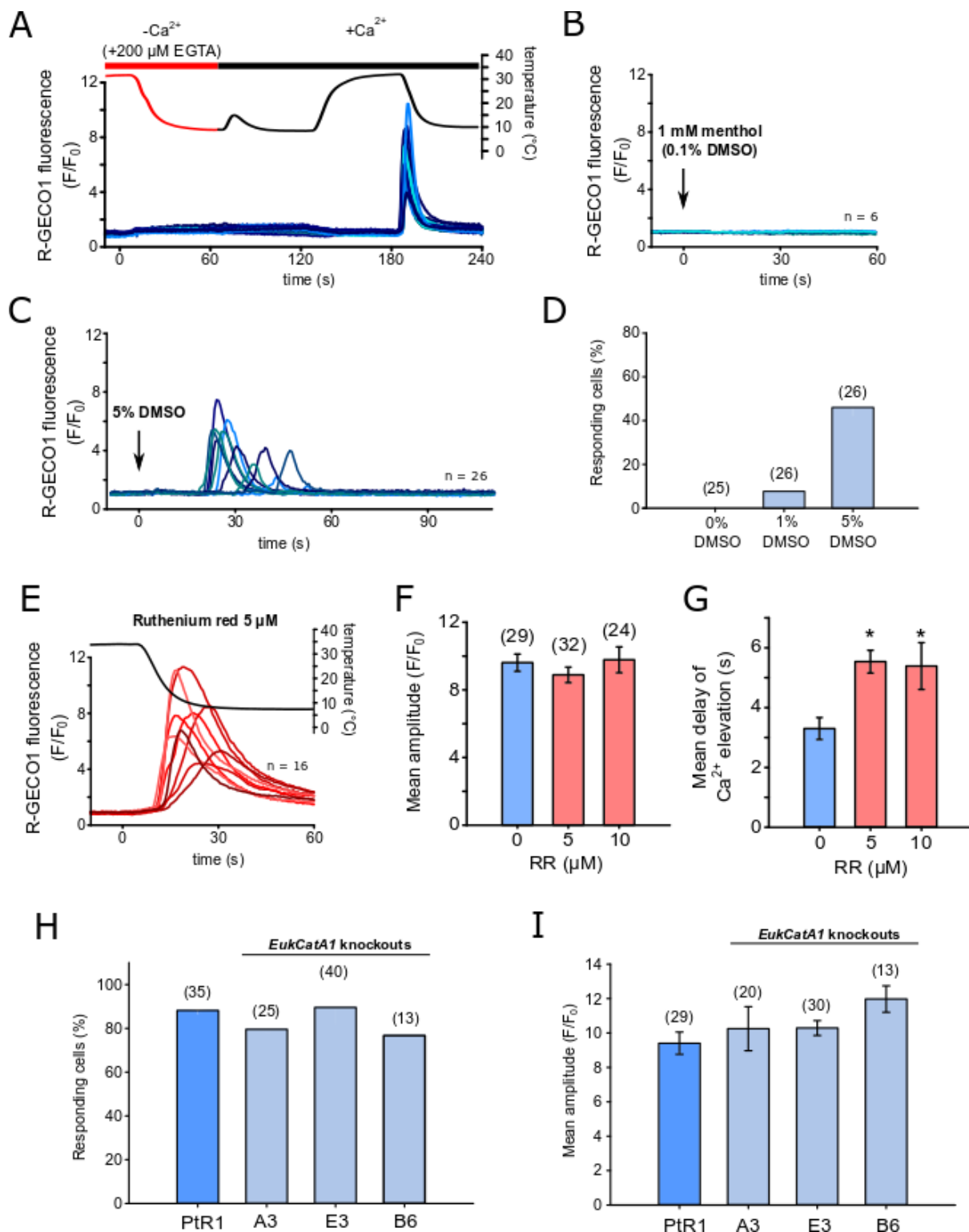
819 image of *T. pseudonana* cells expressing R-GECO1 (yellow) overlaid with chlorophyll

820 autofluorescence (red). Scale bar represents 20  $\mu$ m. E) *P. tricornutum* cold shock response

821 under identical treatment as in A for comparison. F) Percentage of cells exhibiting  $[Ca^{2+}]_{cyt}$

822 elevations. Values in parentheses denote n.

823

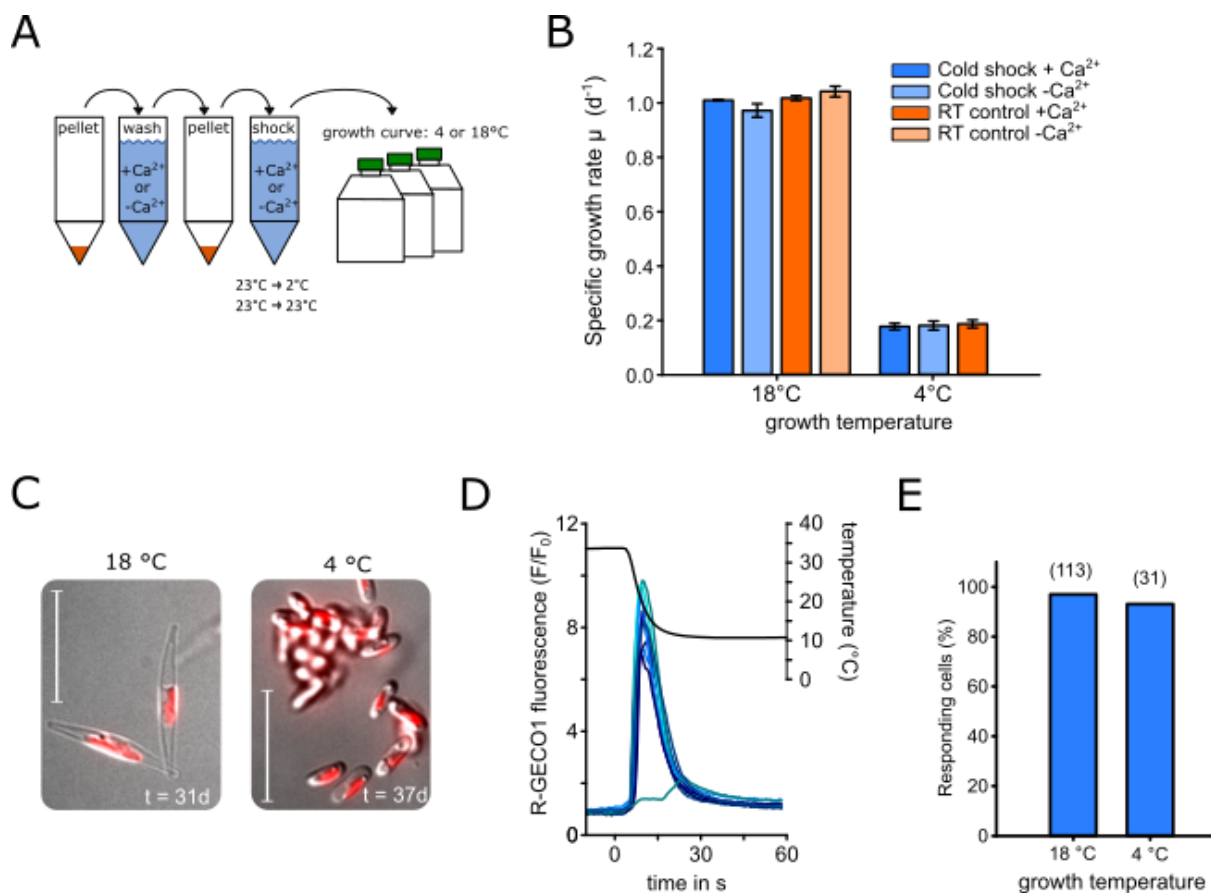


826 **Figure 5: Cellular mechanisms of cold shock induced  $[Ca^{2+}]_{cyt}$  elevations.** A) R-GECO1  
 827 fluorescence ratio ( $F/F_0$ ) from a cold shock applied to PtR1 cells using ASW without  $Ca^{2+}$  +  
 828 200  $\mu M$  EGTA (Methods). No  $[Ca^{2+}]_{cyt}$  elevations can be observed during the cold shock or  
 829 when  $Ca^{2+}$  was restored to cold cells (perfused with cold ASW with  $Ca^{2+}$ ). However,  $[Ca^{2+}]_{cyt}$   
 830 elevations were observed during a subsequent cold shock applied with standard ASW (i.e.

831 with 10 mM CaCl<sub>2</sub>). Note the minor temperature increase at 70 s is due to a slight warming of  
832 cold ASW+Ca<sup>2+</sup> media in the perfusion system. 23 representative traces are shown, three  
833 additional experiments were performed with identical results. **B)** PtR1 fluorescence in  
834 response to ASW containing 1 mM menthol (including 0.1% DMSO as solvent carrier). Six  
835 representative traces are shown. **C)** R-GECO1 fluorescence ratio of PtR1 cells perfused with  
836 ASW + 5% DMSO. **D)** Percentage of cells exhibiting [Ca<sup>2+</sup>]<sub>cyt</sub> elevations in response to  
837 DMSO. **E)** The effect of cold shock on PtR1 cells pre-treated with the Ca<sup>2+</sup> channel blocker  
838 ruthenium red (5 μM final, 5 min pre-incubation). 16 representative traces are shown. **F)**  
839 Mean amplitude (±SE) of responding cells treated with ruthenium red (5 μM or 10 μM)  
840 compared to untreated control cells. No significant differences were observed (one-way  
841 ANOVA). **G)** Mean timing (±SE) of the maximal amplitude of [Ca<sup>2+</sup>]<sub>cyt</sub> elevations for cells  
842 treated with ruthenium red (P = <0.01, one-way ANOVA, Holm-Sidak post-hoc test). **H)**  
843 Percentage of cells showing [Ca<sup>2+</sup>]<sub>cyt</sub> elevations in response to cold shock in control and three  
844 independent *eukcata1* mutant strains (30 to 10 °C). Data represent a minimum of two  
845 independent experiments per strain (one-way ANOVA). **I)** Mean maximal amplitude (±SE) of  
846 [Ca<sup>2+</sup>]<sub>cyt</sub> elevations in *eukcata1* mutants in response to cold shock. No significant differences  
847 were observed (one-way ANOVA on Ranks).

848



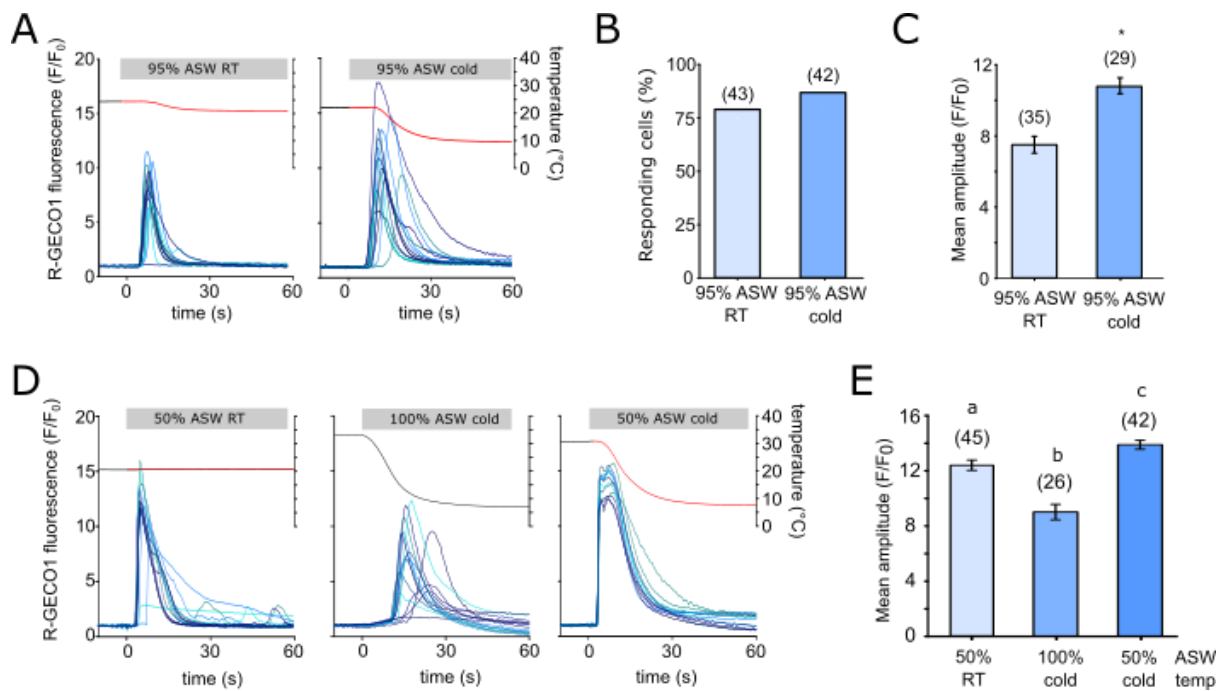


849

850 **Figure 6: The role of the cold shock response in cold tolerance.** **A)** Schematic diagram  
 851 showing the workflow for an experiment examining the impact of Ca<sup>2+</sup>-dependent cold shock  
 852 signalling on *P. tricorutum* cold tolerance. Cells were harvested and washed in ASW  
 853 containing 10 mM Ca<sup>2+</sup> or no Ca<sup>2+</sup> (ASW -Ca<sup>2+</sup> +200 μM EGTA). Cells were pelleted once  
 854 again and exposed to cold shock with or without Ca<sup>2+</sup>. Cells were then grown at control (18  
 855 °C) and cold (4 °C) conditions in standard ASW (i.e. with 10 mM CaCl<sub>2</sub>) to examine cold  
 856 tolerance. **B)** Growth rate of *P. tricorutum* cultures after cold shock treatment. Mean specific  
 857 growth rates were calculated from day 0-5 and 12-30 for 18 °C and 4 °C, respectively. Note  
 858 that for growth at 4 °C, a no shock (RT) control in the absence of Ca<sup>2+</sup> was not included. No  
 859 significant differences were observed between treatments at each temperature (one-way  
 860 ANOVA). Error bars represent SE. **C)** DIC images of PtR1 cells grown at 18 or 4 °C. Oval  
 861 cells predominate in cells grown at 4 C for extended periods. Red = chlorophyll auto-  
 862 fluorescence, bar = 20 μm. **D)** Cold-acclimated PtR1 cells still exhibit a response to cold  
 863 shock. Representative R-GECO1 fluorescence ratio traces from PtR1 cells grown at 4 °C for 4  
 864 days. Cells were briefly warmed to 30 °C before a cold shock was applied. **E)** The percentage  
 865 of cells responding to cold shock as function of acclimation temperature. The results were

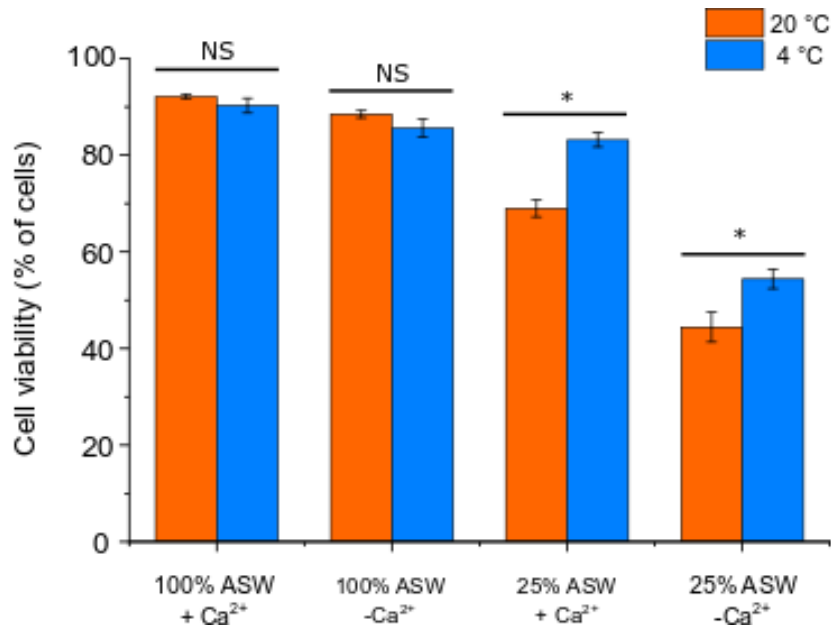
866 generated from four separate experiments with maximum temperature drop-rates between 2.2  
867 - 3.2 C° s<sup>-1</sup>.

868



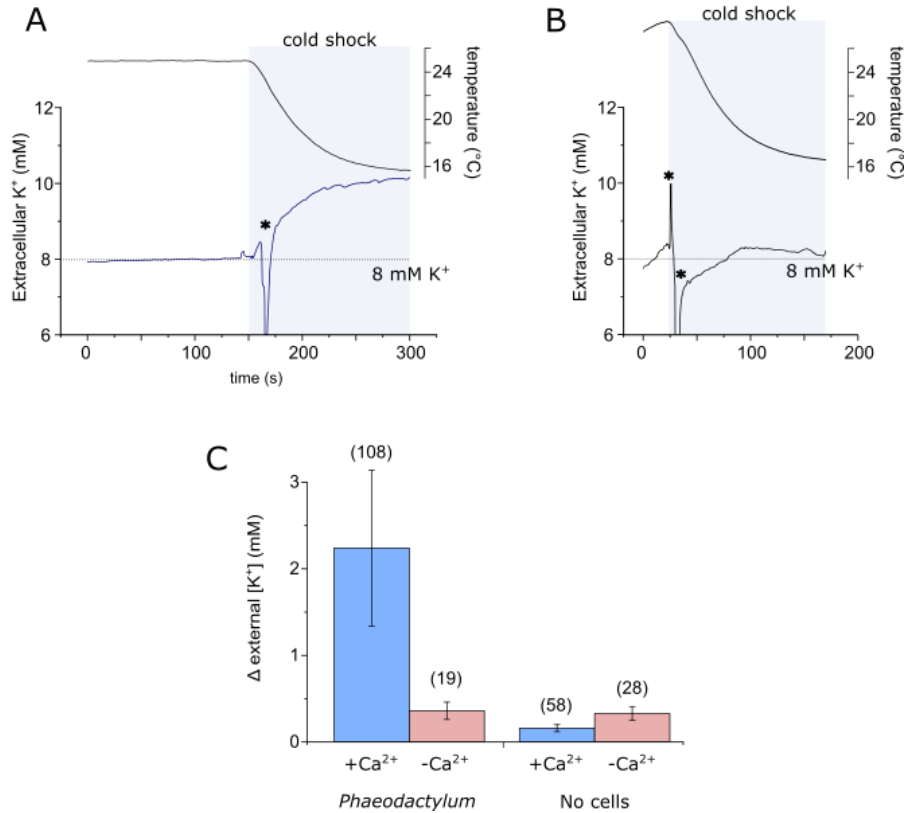
869  
870  
871

872 **Figure 7: Interactions between the cold shock and hypo-osmotic shock  $Ca^{2+}$  signalling**  
873 **pathways.** **A)** R-GECO1 fluorescence ratio ( $F/F_0$ ) of PtR1 cells in response to a mild hypo-  
874 osmotic shock (95% ASW, left panel) or a simultaneous hypo-osmotic and cold shock (10 °C  
875 decrease, right panel). 12 representative traces are shown. **B)** Percentage of cells exhibiting  
876  $[Ca^{2+}]_{cyt}$  elevations for the experiment described in (A). Data are compiled from a minimum  
877 of two independent treatments. **C)** Mean amplitude of  $[Ca^{2+}]_{cyt}$  elevations from responding  
878 cells in (B). The two treatments are significantly different (Student's t-test  $P < 0.001$ ). **D)** R-  
879 GECO1 fluorescence ratio of PtR1 cells in response to stronger simultaneous cold- and hypo-  
880 osmotic shocks. Cells were treated with a single hypo-osmotic shock (50% ASW), a single  
881 cold shock (10 °C) or a simultaneous cold- and hypo-osmotic shock (50% ASW, 10 °C). 13  
882 representative traces are shown. **E)** Mean maximal amplitude of cells exhibiting  $[Ca^{2+}]_{cyt}$   
883 elevations in (D). For biphasic peaks the higher amplitude was chosen. The data represent the  
884 combination of at least three independent experiments per treatment. Letters represent  
885 significant differences between treatments (1-way Kruskal-Wallis ANOVA Ranks  $P < 0.001$ ,  
886 with Dunn post hoc).



887

888 **Figure 8: Simultaneous cold shock reduces mortality associated with hypo-osmotic**  
889 **shock.** Cell viability (measured by exclusion of Sytox Green stain) was determined in *P.*  
890 *tricornutum* cells 3 min after exposure to a severe hypo-osmotic shock (25% ASW) with or  
891 without simultaneous cold shock (4 °C ASW). The presence or absence of external Ca<sup>2+</sup> was  
892 used to establish the effect of inhibiting Ca<sup>2+</sup> signalling during the applied shocks. The  
893 decrease in cell viability due to a hypo-osmotic shock (25% ASW) is significantly reduced  
894 when a simultaneous cold shock is applied. Three replicates were performed for each  
895 treatment, with at least 100 cells counted for each replicate. Significant differences due to  
896 temperature are marked with \* (P<0.05 1-way ANOVA with Holm-Sidak post-hoc test). The  
897 experiment was repeated four times with similar results each time. Error bars represent SE.



898

899

900 **Figure 9: Cold shock induces a Ca<sup>2+</sup>-dependent K<sup>+</sup> efflux.** **A)** K<sup>+</sup> efflux from *P.*  
 901 *tricornutum* cells during a cold shock. A K<sup>+</sup> microelectrode was placed adjacent to densely-  
 902 packed *P. tricornutum* cells to measure K<sup>+</sup> in the immediate vicinity of the cell. A cold shock  
 903 was applied by perfusion. The increase in extracellular K<sup>+</sup> is the result of K<sup>+</sup> efflux from the  
 904 cells. The temperature in the dish is also shown (upper trace). **B)** Extracellular K<sup>+</sup> during a  
 905 cold shock in the absence of external Ca<sup>2+</sup> (perfusion with ASW-Ca<sup>2+</sup> + 200 μM EGTA). **C)**  
 906 Mean change in extracellular K<sup>+</sup> around *P. tricornutum* cells during a cold shock. White bars  
 907 indicate control experiments where the experimental set up was identical, but no *P.*  
 908 *tricornutum* cells were present in order to assess whether the performance of the K<sup>+</sup>  
 909 microelectrode was influenced by temperature. The total number of replicates for each  
 910 treatment are shown in parentheses, error bars = SE.